A relocatable ocean model in support of environmental emergencies

Citation: Dominicis, Michela De, Silvia Falchetti, Francesco Trotta, Nadia Pinardi, Luca Giacomelli, Ernesto Napolitano, Leopoldo Fazioli, et al. "A Relocatable Ocean Model in Support of Environmental Emergencies." Ocean Dynamics 64, no. 5 (April 24, 2014): 667–688.

As Published: http://dx.doi.org/10.1007/s10236-014-0705-x

Publisher: Springer-Verlag

Persistent URL: http://hdl.handle.net/1721.1/98276

Version: Author's final manuscript: final author's manuscript post peer review, without publisher's formatting or copy editing

Noname manuscript No.
(will be inserted by the editor)

A Relocatable Ocean Model in support of environmental emergencies

The Costa Concordia emergency case

Michela De Dominicis · Silvia Falchetti · Francesco Trotta · Nadia Pinardi · Luca Giacomelli · Ernesto Napolitano · Leopoldo Fazioli · Roberto Sorgente · Patrick J. Haley Jr. · Pierre F.J. Lermusiaux · Flavio Martins · George Kallos · Michele Cocco

Received: date / Accepted: date

Abstract *During the Costa Concordia emergency case, regional, sub-regional and relocatable ocean models have been used together with the oil spill model, MEDSLIK-II, to provide ocean currents forecasts, possible oil spill scenarios and drifters trajectories simulations. Their results together with the evaluation of their performances are presented in this paper. In particular, we focused this work on the implementation of the IRENOM (Interactive RElocatable Nested Ocean Model), based on the Harvard Ocean Prediction System (HOPS), for the Costa Concordia emergency and on its validation using drifters trajectories released in the area of the accident. It is shown that thanks to the capability of improving easily and quickly its configuration, the IRENOM results are of greater accuracy than the results achieved using regional or sub-regional model products. The model topography, the initialization procedures and the horizontal resolution are the key model settings to be configured. Furthermore, the IRENOM currents and the MEDSLIK-II simulated trajectories showed to be sensitive to the spatial resolution of the meteorological fields used, providing higher prediction skills with higher resolution wind forcing.*

Keywords relocatable model · trajectory model · drifters

M. De Dominicis
Istituto Nazionale di Geofisica e Vulcanologia, Bologna, Italy
E-mail: michela.dedominicis@bo.ingv.it

S. Falchetti
University of Bologna, Italy

F. Trotta
University of Bologna, Italy

N. Pinardi
University of Bologna, Italy

L. Giacomelli
University of Bologna, Italy

E. Napolitano
ENEA, Rome, Italy

L. Fazioli
CNR-IAMC, Oristano, Italy

R. Sorgente
CNR-IAMC, Oristano, Italy

P.J. Haley Jr.
Massachusetts Institute of Technology, Cambridge, Massachusetts, USA

P.F.J. Lermusiaux
Massachusetts Institute of Technology, Cambridge, Massachusetts, USA

F. Martins
Universidade do Algarve, Faro, Portugal

M. Cocco
Tuscan Archipelago National Park, Portoferraio-Isle of Elba, Italy

George Kallos
University of Athens, Greece

1 Introduction

Relocatable models have been employed for emergency weather predictions, with results very useful for our society in the cases of severe weather outbreaks, hails, tornados and hurricanes (e.g. Schroeder et al, 2006; Bender et al, 2007). In the ocean, tidal and shallow water models were likely the first relocatable models (e.g. [23] [7] [71]), again with multiple societal uses. A pioneer relocatable primitive-equation ocean model was that of the Harvard Ocean Prediction System (HOPS). It was utilized for real-time shipboard predictions of ocean mesoscale circulations for the first time in the Iceland-Faeroe Front region [86]. Subsequently, the HOPS relocatable model and its improved versions were employed to issue real-time forecasts and analyze ocean dynamics in diverse regions of the worlds oceans, including the Atlantic Ionian Stream and Strait of Sicily region [87] [44], the Strait of Gibraltar [89], the Tunisia-Sardinia-Sicily region [68] and the Eastern Ligurian Sea [91]. Starting in the early 2000s, Maritime Rapid Environmental Assessment (MREA, [89]) became one of the drivers for relocatable ocean modeling and forecasting. Such applications required evaluating the usefulness of predictions, especially the assessment of the predictive capability [90] of the modeling systems. With this basis, more rigorous evaluations were completed in 2003 and 2004, for the relocatable Mini-HOPS modeling system applied to the Elba region and off the coast of Portugal [49]. A relocatable modeling approach for MREA04 has been also applied off the coast of Portugal [38]. The relocatable HOPS system has been also integrated with the ocean general circulation model of the Mediterranean Forecasting System (MFS) [93]. A review of the MREA concepts and applications is provided in Ferreira-Coelho and Rixen (2008) [27]. Relocatable models were also employed recently for studying Lagrangian dynamics and dispersion in the Gulf of Mexico region [108], which is an application related to our research.

Oil slicks caused by oil tanker/ships accidents compose a major source of hydrocarbon pollution for the marine and coastal environment *(including seagrass beds, mangroves, algal flats, coral reefs) and can jeopardize the functional integrity of the marine ecosystem (seabirds populations, fish communities, marine mammals) [34] [73] [72]. Since oil spill evolution depends on the winds, waves, sea temperature and current conditions, oil spill management strategies need to be developed together with the improvement of meteorological, ocean and wave forecasting models.*

Pioneer examples of an oil spill response system were available during the Braer oil spill (Shetland Islands, UK, 1993) [77] and the Erika oil spill (Brittany coast in the Bay of Biscay, France, 1999) [18], which for the first time allowed operators to develop a response strategies rather than react only to observed information. Further examples of operational forecasting system for developing proper response strategies to oil spill emergencies were available during the Prestige oil spill crisis (Galicia coast, Spain, 2002) [12] [13] [46]. In the Mediterranean Sea, an oil-spill decision-support system was developed during the largest oil-release accident in the Eastern Mediterranean, the Lebanese

oil-pollution crisis, which occurred in mid-July 2006 [15]. During the recent largest accidental marine oil spill in the history of the petroleum industry, effective oil spill monitoring and modeling systems were critical to the rapid responses achieved for the Deepwater Horizon event (Gulf of Mexico, 2010). The value of regional models (with improved resolution and topography) was demonstrated [57] and an ensemble forecast system has been developed with a focus on regional and global scales [51] [52]. An example of a quasi-operational forecasting system composed by a finite-element model and a particle-tracking model was also implemented to provide high-resolution current velocity field and surface trajectories of the oil on the continental shelf and nearshore [24]. However, the majority of the above oil spill rapid response systems were based on regional or even basin-scale models. Thus, there is a need to analyze the possibility to use relocatable models, that can be rapidly implemented in any region of the world, and to asses if they can provide accurate forecasts in a very short time, as required by the management of emergencies produced by oil spills or contaminants releases at sea.

An oil spill model is an important component in any emergency response or contingency plan. Oil spill numerical modeling started in the early eighties and, according to state-of-the-art reviews [5] [80], a large number of numerical Lagrangian surface oil spill models have growth in the last 30 years. These models can vary from simple point source particle-tracking models, such as TESEO-PICHI [13] [98], to complex models that attempt to comprehensively simulate the three-dimensional advection-diffusion-transformations processes that oil undergoes [107] [106]. Some of the most sophisticated Lagrangian operational models are COZOIL [79], SINTEF OSCAR 2000 [82], OILMAP [99, 4], GULFSPILL [1], ADIOS [43], MOTHY [19], MOHID [12], the POSEIDON OSM [74, 65], OD3D [29], the Seatrack Web SMHI model [3], MEDSLIK [41, 42], GNOME [112], OILTRANS [10] and MEDSLIK-II [21]. Which type of model to use depends on the model availability in the area of interest and end objectives: from short-term forecasting to long-term impact assessment. The oil spill model used in this work is MEDSLIK-II [21], that is able to simulate the transport of surface drifters or the transport, diffusion and transformations of a surface oil slick. It has been used extensively in the past to simulate oil spill accidents [15] and/or drifter trajectories [22] and it proved to be reliable in short-term forecasting.

On January 13th, 2012 the Costa Concordia cruise ship hit a rocky outcrop and ran aground rolling onto its side as it sailed near the Giglio island. With 2500 tons of fuel in its tanks, the Coast Concordia was immediately considered a high risk accident for possible spills to occur. Though hypothetical, an oil spill scenario could not be totally discarded. *MEDSLIK-II has been connected to operational regional (MFS, [75]) and sub-regional models, the Western Mediterranean (WMED) [67] and the Tyrrhenian Sea (TYRR) [105], to simulate scenarios of fuel leaks. In Fig. 1 the geographical domains of the models are presented. The oil spill scenarios and current forecasts have been provided every day and in real time to the Italian Coast Guard. In case of an oil spill, this information would have helped to plan the booms deploy-*

ment, to place skimmers, to protect a particular piece of coast or to intervene with airplanes or vessels. Moreover, a high resolution, relocatable model, called IRENOM (Interactive RElocatable Nested Ocean Model) has been nested in MFS and its currents used as input to the MEDSLIK-II model. The hydrodynamics model core of IRENOM is based on the Harvard Ocean Prediction System (HOPS) [88] and the area of interest of this work is the north-eastern Mediterranean Sea where the Costa Concordia accident occurred (see Fig. 2).

To assess the accuracy of the oil spill simulations and of the ocean current predictions, *a validation experiment with the release of four I-SPHERE drifters has been performed* in the area of the accident. MEDSLIK-II has been used to simulate the drifter trajectories using the current fields output from different operational oceanographic models and from IRENOM. The latter has been shown to produce realistic drifter trajectories with higher accuracy than the coarser resolution regional and sub-regional models. In this work, the improvements in having high resolution and accurate forecasts of the ocean currents will be assessed and the sensitivity of the drifter trajectory forecasts to model configuration parameters will be analyzed.

The manuscript is organized as follows: section 2 overviews the hydrodynamic models and oil spill model, together with the drifters data used for the validation, section 3 shows the results of the operational support provided during the emergency, section 4 presents the results of the IRENOM implementation and drifters validation experiments and section 5 offers the conclusions.

2 Models and data

2.1 IRENOM - Interactive RElocatable Nested Ocean Model

The relocatable IRENOM ocean model is based on the hydrodynamics core model of HOPS [88], an integrated system of software for multidisciplinary oceanographic research developed by the physical oceanography group of Harvard University. As mentioned earlier, HOPS has been used in varied ocean regions for real-time ocean forecasting, data assimilation and dynamics studies, especially in the Mediterranean Sea [87] [44] [89] [68] [91]. The initial version of the primitive-equation (PE) model of HOPS was a rigid-lid code, initialized based on procedures described in Lozano et al. (1996) [55] and Robinson et al. (1996) [86]. Since that time, a free-surface version of HOPS was developed, numerical schemes were updated and new algorithms were developed. This led to a new conservative finite-volume structured ocean model code with implicit two-way nesting for multiscale hydrostatic PE dynamics with a nonlinear free-surface [30]. With this Multidisciplinary Simulation, Estimation and Assimilation System, some of the modeling capabilities include: balanced and nesting initialization and downscaling [31]; multi-resolution data-assimilative tidal prediction and inversion [54]; fast-marching coastal objective analysis [2];

stochastic subgrid-scale models (e.g., [45]); and data assimilation and adaptive sampling [47].

In this manuscript, the core of the HOPS code employed is a free-surface, primitive-equation model and the prognostic variables are sea level, temperature, salinity and total velocity discretized on an Arakawa B grid. The vertical coordinate adopted is a topography-following system, in particular a double-sigma system, chosen for accurate modelling of steep topography and the surface mixed layer. In the present set-up of HOPS, we use lateral open boundary conditions given in terms of an Orlanski [70] radiation condition, applied to temperature and salinity and velocity components. For sea level a zero gradient boundary condition is chosen. The precipitation values are taken from climatologically monthly dataset CPC Merged Analysis of Precipitation (CMAP) [111]. The surface heat and momentum fluxes are calculated interactively by the model from meteorological fields (see Sect. 2.3) using bulk formulae.

In this work, initial and lateral boundary conditions for IRENOM are taken only from the operational Mediterranean Forecasting System (MFS) model [66] described later in Sect. 2.3. The variable temperature, salinity and the total velocity are extracted from MFS daily mean and hourly fields and bilinearly interpolated onto the horizontal HOPS grid and mapped from flat (z-levels) to terrain-following levels.

The IRENOM is configured trough an user friendly Graphical User Interface (GUI). Fig. 3 shows the flowchart of the IRENOM implementation trough the GUI. After the acquisition of the necessary input forcings (*MFS currents and ECMWF or SKIRON winds, see Sect. 2.3*) for the selected period, the GUI software executes two simultaneous processes: the generation of the grid and the input data conversion into IRENOM format. The preparation of the grid is divided into various phases. First, the horizontal grid is defined on the basis of the coordinates and resolution indicated by the user. Then, *trough the GUI* the user can choose different positions of the vertical levels by varying some parameters, such as shallowest depth to retain (vertical clipping), number of levels or the slope. The vertical grid and the land-sea mask are generated automatically. The user may also manually change the default land-sea mask *by using the GUI*, i.e. introduce or remove islands in the domain, depending on the resolution to be achieved or the physical processes to be resolved. Then, the interpolation of the father model currents on the IRENOM grid is performed to generate the initial condition and boundary conditions. At this point the simulation can be performed. At the end of the simulation, the GUI allows the visualization of the results, the transformation of the output in different formats and the model diagnostics.

Before describing the oil spill model (Sect. 2.2), we note that downscaling and nesting of different regional models has been successfully completed before (e.g. [69] [78] [48]). In our case, even though we employ a 1-way nesting scheme for the downscaling of the operational Mediterranean Forecasting System, 2-way nesting could have been used. For a review on nesting schemes, we refer to Debreu and Blayo (2008) [25]. Recent nesting schemes relevant to our application are obtained in Haley and Lermusiaux (2010) [30] and Mason et al

(2010) [58]. In particular, the implicit 2-way nesting of Haley and Lermusiaux (2010) could be combined with nesting initialization and downscaling schemes [31] which improve the consistency among model fields and reduce unphysical transients due to nesting of multiple model types.

2.2 The oil spill and trajectory model: MEDSLIK-II

The oil spill model code MEDSLIK-II [21,22] is now a freely available community model [59]. It is designed to be used to predict the transport and weathering *(evaporation, dispersion, spreading and beaching, as described in [21])* of an oil spill or to simulate the movement of a floating object. MEDSLIK-II is a Lagrangian model, which means that the oil slick is represented by a number N of constituent particles that move by advection from the hydrodynamics currents and disperse horizontally by Lagrangian turbulent diffusion. The horizontal current field used in the Lagrangian model is taken to be the sum of different components:

$$\begin{aligned} d\mathbf{x}_k(t) = [&\mathbf{U}_C(x_k, y_k, t) + \mathbf{U}_W(x_k, y_k, t) + \mathbf{U}_S(x_k, y_k, t) \\ &+\mathbf{U}_D(x_k, y_k, t)]\, dt + d\mathbf{x}'_k(t) \end{aligned} \tag{1}$$

where $\mathbf{U}_C$ is the wind, buoyancy and pressure driven large scale current velocity field, $\mathbf{U}_W$ is the local wind velocity correction term, $\mathbf{U}_S$ is the wave-induced current term (Stokes drift velocity), $\mathbf{U}_D$ is the wind drag correction due to emergent part of the objects at the surface and $d\mathbf{x}'_k(t)$ is the displacement due to the turbulent diffusion. The local wind correction term $\mathbf{U}_W$ and the Stokes drift $\mathbf{U}_S$, are written as:

$$\begin{aligned} U_W &= \alpha(W_x \cos\beta + W_y \sin\beta) \\ V_W &= \alpha(-W_x \sin\beta + W_y \cos\beta) \end{aligned} \tag{2}$$

$$\begin{aligned} U_S &= D_S \cos\vartheta \\ V_S &= D_S \sin\vartheta \end{aligned} \tag{3}$$

where (W_x, W_y) are the wind velocity components at 10 m, $\vartheta = arctg\left(\frac{W_x}{W_y}\right)$ is the wind direction and D_S is the Stokes drift velocity intensity in the direction of the wave propagation at the surface, defined as:

$$D_S(z=0) = 2\int_0^\infty \omega k(\omega) S(\omega) d\omega \tag{4}$$

where ω is angular frequency, k is wave-number, and $S(\omega)$ is wave spectrum. Using this parametrization we assume that wind and waves are aligned and the waves are generated only by the local wind (swell process is not considered).

When $\mathbf{U}_C$ is provided by oceanographic models that resolve the upper ocean layer dynamics (1-3 m resolution and turbulence closure sub-models), the term $\mathbf{U}_C$ contains a satisfactory representation of surface ageostrophic

currents and the $\mathbf{U}_W$ term may be neglected (in this work $\mathbf{U}_W$ has been always set equal to 0). The wind drag correction, $\mathbf{U}_D$, is associated with the leeway (windage) of a floating object, defined as the drift associated with the wind force on the overwater structure of the object. As defined by [92] and [33] the leeway-drift velocities can be parametrized as follows:

$$\mathbf{U}_D = \sqrt{\frac{\rho_a}{\rho_w}\frac{A_a}{A_w}\frac{Cd_a}{Cd_w}}\mathbf{W} = \gamma\mathbf{W} \tag{5}$$

where ρ, A, C_d are the fluid density, projected areas of the object and drag coefficient, respectively, and subscripts a and w denote the air and seawater environments. The parameter γ cannot be calculated directly because the drag coefficients Cd_a and Cd_w are Reynolds numbers dependent and are not straightforward to use at the air-sea interface with wave disturbances [92]. Field experiments performed by [92] suggest to use γ in the range 0.003 - 0.01. In the simulation experiments of single drifter trajectories (see Sect. 4), γ has been set equal to 0.01 thus, $\mathbf{U}_D$ is about 1% of the wind velocity. While simulating real oil slick (see Sect. 3) the leeway-drift velocity has been omitted, $\mathbf{U}_D = 0$.

The turbulent diffusion is parameterized with a random walk scheme as

$$d\mathbf{x}'_k(t) = \sqrt{2\mathbf{K}dt}\ \mathbf{Z} \tag{6}$$

where $\mathbf{K}$ is the turbulent diffusion diagonal tensor and $\mathbf{Z}$ is a vector of indipendent random numbers used to model the Brownian random walk processes chosen for the parametrization of turbulent diffusion. The turbulent diffusion is considered to be horizontally isotropic and the three diagonal components of $\mathbf{K}$ are indicated by K_h, K_h, K_v. In the simulation experiments of a real oil slick (see Sect. 3), K_h has been set to $2\,\mathrm{m^2s^{-1}}$, in the range $1 - 100\,\mathrm{m^2s^{-1}}$ indicated by [5] and [20], while K_v has been set to $0.01\,\mathrm{m^2s^{-1}}$ in the mixed layer (assumed to be 30 m deep) and below it to $0.0001\,\mathrm{m^2s^{-1}}$. When simulating single drifter trajectories (see Sect. 4) the diffusivity coefficients are set to zero.

When simulating a real oil slick, MEDSLIK-II allows the processes of spreading, evaporation, dispersion, emulsification and coastal adsorption to evolve. When the oil first enters the sea, the slick spreads on the sea surface because of gravitational forces. As it is transported, lighter oil components disappear through evaporation and heavier ones emulsify with the water or are dispersed in the water column. MEDSLIK-II is also able to take into account adsorption of oil by the coast should the slick reach it. The full description of the model formulation can be found in [21].

2.3 The larger scale current models and the atmospheric forcing

By way of inputs, both IRENOM and MEDSLIK-II require data on sea currents, sea surface temperature and atmospheric forcing. For the ocean currents,

MEDSLIK-II has been connected to regional (MFS, [75]) and subregional operational current models, such as the Western Mediterranean (WMED) [67] and the Tyrrhenian Sea (TYRR) [105]. Furthermore, IRENOM has been nested in MFS and MEDSLIK-II used as input the IRENOM currents to examine the trajectory simulations skill of the relocatable model with respect to all the others. *The main characteristics of the OGCMs presented in this Section are listed in Tab. 1 and geographical domains are shown in Fig. 1.*

The MFS system [63] is composed of an OGCM [66] covering the entire Mediterranean Sea and an assimilation scheme [26] which corrects the model's initial guess with all the available in situ and satellite observations. The model code is NEMO (Nucleus for European Modelling), a detailed description of the code can be found in Madec et al. (2008) [56]. NEMO is coupled with the wave model WWIII (WAVEWATCH III, [102] [17]). NEMO and WWIII have been implemented in the Mediterranean at 1/16° (approximately 6.5 km) horizontal resolution and 71 unevenly spaced vertical levels. *The model is forced by momentum, water and heat fluxes interactively computed by bulk formulae using the 6-hourly, 0.25° horizontal-resolution operational analyses from the European Centre for Medium-Range Weather Forecasts (ECMWF) and the model predicted surface temperatures (details of the air-sea physics are in Tonani et al., 2008 [103]).* Operationally, MFS produces daily and hourly mean forecasts. Once a week, the system also provides daily mean and hourly analyses, which are best estimates of oceanographic conditions. The MFS basin scale output provides initial and lateral boundary conditions for higher resolution sub-regional models in addition to MFS.

WMED [110] is a three-dimensional primitive equation hydrodynamic model based on the Princeton Ocean Model (POM, [8]). POM solves the equations of continuity, motion, conservation of temperature, salinity and assumes hydrostatic and Boussinesq approximation. WMED covers the western Mediterranean area (from 3.0° E to 16.47° E in longitude and from 36.7° N to 44.48° N in latitude) with a horizontal grid resolution of 1/32° (approximately 3.5 km). In the vertical it uses 30 sigma levels, denser at the surface following a logarithmic distribution. The model is initialized with a cold start using dynamically balanced forecast fields from MFS, through a downscaling of the forecast fields produced by the basin-scale circulation models. In this case, the forecasts result to be closely dependent on the accuracy of the MFS fields and on the methodology used for interpolating the regional-scale model on the model numerical grid (horizontal and vertical). This method of initialization is also known as a slave mode forecasting mode. The main disadvantage of this methodology has to do with the different resolutions, both horizontal and vertical, of the regional and basin-scale models. Incorrect dynamic balancing of interpolated fields leads, in fact, to the generation and propagation of gravity waves during the spin-up time [6]. To minimize this noise in the downscaling procedure, a best-interpolation method based on VIFOP (Variational Initialization and Forcing Platform) variational analysis is used [28]. MFS also provides boundary conditions through a simple off-line one way asynchronous nesting as described in details in Sorgente et al. (2003) [97]. Surface fluxes are com-

puted through bulk formulas [14] from the 6-hourly atmospheric analyses from ECMWF at 0.25° of resolution. WMED provides a daily 5-day prediction of water currents, temperature and salinity at different water depths as daily and hourly mean output.

TYRR [101] is one of the nested models covering the area of Tyrrhenian Sea (from 8.81°E to 16.29°E in longitude and from 36.68°N to 44.50°N in latitude) with a horizontal grid resolution of 1/48° (approximately 2 km). The numerical model used is Princeton Ocean Model (POM) [8] [61]. *The vertical grid consists of 40 sigma levels that are smoothly distributed along the water column, with appropriate thinning designed to better resolve the surface and intermediate layers. Initial conditions are taken from MFS analysis as follows: every week an hindcast run of 7 days is performed, it is forced by the ECMWF analysis fields and uses the MFS analysis fields for initial and boundary conditions. After this spin-up period of 7 days, for the following week the TYRR system provides a daily 5-day prediction of water currents, temperature and salinity at different water depths as daily and hourly mean output, starting from the restart of the forecast of the day before.* Boundary conditions are obtained by interpolating on the TYRR grid the temperature, salinity, velocities, and surface elevation fields produced by the MFS.

For the atmospheric forcing, a sensitivity analysis of the IRENOM currents and the MEDSLIK-II trajectory simulation skills to the meteorological fields resolution has been performed. The first atmospheric forcing used comes from the ECMWF model output (0.25° and 6 hours), which is the forcing used operationally by the regional, MFS, and sub-regional models, WMED and TYRR. The second one is the higher resolution atmospheric model SKIRON, with 0.025° horizontal resolution and temporal frequency of 1 hours (6hours). SKIRON [100] is a modeling system developed at the University of Athens from the AM&WFG [36] [37]. The atmospheric model is based on the ETA/National Centers for Environmental Prediction (NCEP) model, which was originally developed by Mesinger [62] and Janjic [35] at the University of Belgrade. Details on the various model parameterization schemes can be found in the above mentioned studies and references therein.

2.4 Drifters data

The drifters are oceanographic instruments used to study the surface circulation and oceanographic dynamics, they are designed to be transported by ocean currents and these characteristics make them useful tools for the validation hydrodynamic models [9] [32] [50] and oil spill/trajectory models [81] [1] [76] [11] [98] [16] [53] [57]. Oil spill-following surface drifters (i-SPHERE) [76] are 39.5 cm diameter spheres designed on the basis of earlier experiments carried out in the late 1980s and early 1990s.

During the Costa Concordia emergency, drifters were deployed south-eastward of the Giglio island (Fig. 4). The 4 drifters were released the 14 of February 2012 and recovered 24 hrs later. As shown in Fig. 4, the buoys had a linear

arrangement from northeast to southwest and an average distance of about 7 km between Giglio and Giannutri Island. These data were used to evaluate the accuracy of the ocean currents provided by MFS, WMED, TYRR. Then, the drifters were used to validate the different IRENOM model settings, in order to understand the improvements in simulating the ocean state derived from a nested relocatable model approach.

2.5 Lagrangian trajectory evaluation metrics

Two metrics will be used to quantitatively evaluate the accuracy of the Lagrangian trajectory simulations. The first metric is the Lagrangian separation distance $d_i(\mathbf{x}_s(t_i), \mathbf{x}_o(t_i))$ between the observed and the simulated trajectories, where d_i is the distance at the selected time t_i, after a reference time t_0, between the simulated drifter position, $\mathbf{x}_s$, and the observed positions, $\mathbf{x}_o$. The second metric is the Liu (2011) skill score [50]. It is defined as an average of the separation distances weighted by the lengths of the observed trajectories:

$$s(t_i) = \frac{\sum_{t=t_0}^{t_i} d_i(\mathbf{x}_s(t), \mathbf{x}_o(t))}{\sum_{t=t_0}^{t_i} l_{oi}(\mathbf{x}_o(t_0), \mathbf{x}_o(t))} \tag{7}$$

where l_{oi} is the length of the observed trajectory at the corresponding time, t_i, after a reference time t_0. Such weighted average tends to reduce the evaluation errors that may rise using only the purely Lagrangian separation distance. The s index can be used to define a model skill score:

$$ss(t_i) = \begin{cases} 1 - \frac{s(t_i)}{n} & (s \leq n) \\ 0 & (s > n) \end{cases} \tag{8}$$

where n is a tolerance threshold. In this work, as suggested by [50], we used $n = 1$, this corresponds to a criterion that cumulative separation distance should not be larger than the associated cumulative length of the drifter trajectory. The higher the ss value, the better the performance, with $ss = 1$ implying a perfect fit between observation and simulation and $ss = 0$ indicating the model simulations have no skill.

3 The operational support during the emergency: the multi-model approach

On January 13th, 2012, only hours after leaving the Italian port of Civitavecchia, the Costa Concordia cruise ship with more than 4200 passengers and crew on board, hit a rocky outcrop, ran aground and rolled onto its side as it sailed off the island of Giglio. Italian Authorities (Coast Guards and Civil Protection) immediately reacted by deploying Search and Rescue and risks mitigation measures, including environmental risks. With about 2500 tons of fuel in its tanks, questions immediately raised about the potential environmental impact

if the fuel de-bunkering operation fails. A spillage would pollute the Tuscan Archipelago National Park, a marine environmental protected area. Every day, starting from the 16th of January and until the fuel unloading operations finished, the coupled hydrodynamics and MEDSLIK-II system was run to produce scenarios of the possible oil spill from the Costa Concordia. MEDSLIK-II used the currents (hourly fields) provided by the operational ocean models available in the area: MFS, TYRR and WMED. Thanks to these daily data a fuel leak can be simulated to forecast the possible fuel dispersion into the sea and along the coast. The position of the possible oil spill coincides with the ship position in the proximity of Giglio Island harbour. The amount of oil spilled was decreased on the basis of the quantity de-bunkered. Daily bulletins were provided to the Italian Coast Guard Operational Centre. Those bulletins presented the forecasts of the currents, wind and oil dispersion at surface up to 72 hours after the possible spill, supposed to be released continuously in 72 hours. Though hypothetical, an oil spill scenario could not be totally discarded and this information would have been crucial for helping local Maritime authorities to be better prepared in setting up prevention measures and optimising cleaning operations. The bulletin dissemination to other competent authorities was managed and under the responsibility of the Italian Coast Guard and it complemented the information coming from European services (e.g. oil spill detection and monitoring from EMSA, the European Maritime Safety Agency).

Fig. 5 shows an example of the information contained into the bulletin provided to the competent authorities. When all the models are in agreement, we might be more confident in the accuracy of the forecasts. Nevertheless, there were times in which the three models gave very different predictions, as shown in Fig. 5. Reasons for the different model forecasts may be due to the different *numerical code* (NEMO, POM), to the specific grids, parametrizations, data assimilation schemes and domains. Commonalities are that both WMED and TYRR are nested into MFS, but using different initialization procedure (see Sect. 2.3). WMED with a daily initialization from MFS, cannot deviate much from MFS, while TYRR model uses an initialization period of 7 days, allowing the model to produce its own dynamics. *During the Costa Concordia emergency, only a qualitative comparison of the model results has been performed and the different forecasts are not produced from true ensemble prediction systems based on dynamics. Despite this, a similar methodology was implemented during the Deepwater Horizon oil spill [52] [53] and it has demonstrated to provide some degree of confidence that any single model alone might not. Although super-ensemble techniques for ocean [85] and weather forecasting [39] [40] are widely used, few examples on using ocean ensembles in Lagrangian trajectory models are available. It has been demonstrated that the trajectories ensemble can generate important uncertainty information in addition to predicting the drifter trajectory with higher probability, in contrast to a single ocean model forecast [109]. How to combine models results is not a priori obvious and some recent works have been done on this issue. One methodology is the hyper-ensemble technique [83] [84] [104], which combines multiple model of different physical processes (ocean currents, winds, waves) and then perform*

the trajectory simulations using the combined product. The optimal combination is obtained during a training period by minimizing the distance between modelled and observed trajectories and requires comprehensive observational networks. Another option is to combine a posteriori the modelled trajectory obtained using the different velocity fields [94]. In the future and with a larger drifters dataset these methodologies will be explored.

Giving the errors inherent to any model, its forcing fields and its initialization, a validation exercise was organized to assess the quality of produced forecasts, as described in Sect. 2.4. As shown in Tab. 3, nine simulations were done to evaluate the models performances and the sensitivity of the oil spill model to some parametrizations and to the forcing fields. We performed a first set of simulations using only the hourly surface currents, $\mathbf{U}_C$ term of Eq. 1, from MFS, TYRR and WMED. Then, we carried out a second set of experiments to take into account the Stokes drift effect, $\mathbf{U}_S$ term of Eq. 1. The last set of simulations has been performed adding also the wind drag correction, $\mathbf{U}_D$ term of Eq. 1, which is equal to 1% of the wind velocity intensity. In Fig. 6 the comparison between one of the real drifters trajectories (Buoy 1 of Fig. 4) and the simulated trajectories is shown. Qualitatively, we can see that the simulated trajectories using MFS and WMED go in the wrong direction. Using TYRR currents the simulated trajectory are in better agreement with the observed one, but without adding the wind drag correction and the Stokes drift correction (Fig. 6-a and Fig. 6-b) the displacement of the simulated drifter is underestimated. The best results are obtained with the experiment TYRR-CSD (Fig. 6-c), that shows an higher displacement in the correct direction of the simulated drifter. The separation distance, d_{24h}, and the skill score, ss_{24h}, after 24 hours of simulation have been calculated for all buoys. In Tab. 3, the values obtained for Buoy 1 are listed, together with the average over the 4 buoys. Exp. TYRR-CSD shows the lowest separation distance (4.15 km) and highest skill score (0.59) in reproducing Buoy 1 trajectory, confirming that the best results are obtained using the TYRR currents and using the Stokes drift and wind drag terms. In Fig. 7, it is shown the decomposition of the total velocity that drives the simulated Buoy 1 in the Exp. TYRR-CSD. It is found that the effect of the wave correction, $\mathbf{U}_S$, and wind drag correction, $\mathbf{U}_D$, can be, as in this case, of the same order of magnitude of the current velocity, $\mathbf{U}_C$.

4 Validation of the relocatable model using drifters trajectories

During the Costa Concordia emergency, the IRENOM relocatable model has been used in order to provide high/very high-time and space resolution forecasts starting from operational large-scale circulation models. The sensitivity of the relocatable model implementation to some model settings, summarized in Tab. 4, is analyzed and the results are validated using the surface drifters.

In order to test the sensitivity to different horizontal grid resolutions, two horizontal domains are chosen. The first domain covers the region from 41.26°N to 43.93°N and from 9.11°E to 12.73°E. The horizontal grid resolu-

tion is approximately 3 km and consists of 100x100 points. The second domain covers the region from 41.70°N to 43.12°N and from 9.39°E to 12.29°E. The horizontal grid resolution is approximately 2 km and consists of 120x80 points. The two domains are referred in Tab. 1 and Tab. 4 as $HG1$ and $HG2$ respectively and are shown in Fig. 2. Both configurations have 25 double sigma levels. The bathymetry for both configurations has been obtained from the U.S. Navy unclassified 1 minute bathymetric database DBDB-1, by linear interpolation of the depth data into the model grid.

One of the main differences between the IRENOM configurations and MFS is the topography. Due to the low resolution of the MFS model the Giglio Island is not reproduced in the MFS topography, while in the IRENOM model the land/sea mask has been correctly implemented. Thus, it is necessary to initialize the IRENOM model some days before the day of the deployment of the drifters, to let the model correctly reproduce the dynamic of the current between the islands, which drives the drifters transport. The sensitivity to the initialization time (spin-up time) is extensively examined in this work. The spin-up time is defined as the time needed by an ocean model to reach a state of physical equilibrium under the applied forcing. The results cannot be trusted until this equilibrium is reached due to spurious noise in the numerical solution. The sensitivity to a model initialization of 3, 5 and 7 days is tested as indicated in Tab. 4, where these spin-up times are labelled $T11$, $T09$, $T07$ respectively.

Next, in order to test the influence of the topography on the model results, a simulation with alternating direction Shapiro filters is done, see label YS in Table 4. In this case a 4th order Shapiro filter is applied and the number of filter applications is set to 2. The model sensitivity to the shallowest allowed topography is also tested by using a topography clipping value of 5 m (see label $C5$ in Tab. 4) against the standard 10 m value used for all the other model runs.

The above runs were performed using the ECMWF model output with 0.25° resolution, which is the forcing used operationally by MFS, WMED and TYRR. Such coarse atmospheric model gives forcing only every approximately 12x12 grid points of the IRENOM model with 2 km resolution and it might not give a realistic representation of the wind field forcing for a high resolution hydrodynamic model. Thus, a sensitivity analysis of the 2 km configuration of IRENOM model to the horizontal resolution wind forcing has been performed by running IRENOM forced by the SKIRON winds with a resolution of 0.025°. The experiments are indicated in the Tab. 4 with the label SKI. In theory, higher resolution wind forcing should give better predictions, but it is not obvious because if the higher resolution forcing do not represent well the smaller weather scales, island structure, etc., the fine-grid ocean simulation with higher resolution forcing may be worse than with the coarse forcing.

Finally, the 4 buoys were simulated using the MEDSLIK-II model forced by the currents coming from the *11* different IRENOM configurations. The trajectory simulations were performed using the currents, the Stokes drift and the wind drag, because, as it was found in Sec. 3, $\mathbf{U}_S$ and $\mathbf{U}_D$ should not

be neglected. *To be consistent with the IRENOM current fields,* $\mathbf{U}_S$ *and* $\mathbf{U}_D$ *are calculated by MEDSLIK-II using the same wind forcing used to force the IRENOM model.*

Fig. 8-a-b-c shows the IRENOM sea surface current fields obtained with an horizontal resolution of 3 km, ECWMF 0.25° wind forcing and with a spin-up time of 7 (panel a), 5 (panel b) and 3 (panel c). A greater spin-up time causes the developing of stronger currents especially south of Elba island and finer spatial scales have a greater time to develop, as is the case of the circulation pattern north of Elba island. To decide which spin-up time should be used, the general practice [95] would suggest to choose the spin-up time which allows the ocean model to reach a state of physical equilibrium, i.e. TKE plateau reached. Fig. 9 shows the ratio between the Total Kinetic Energy (TKE), on the target day 14 February at 12:00 UTC, of the relocatable model and that of the father model MFS as a function of the spin-up time. The IRENOM model with 3 km of resolution does not reach a plateau, as shown in Fig. 9 (blue line), but the slope of the curve diminished between 5 and 6 days of spin-up time. This behavior would suggest better trajectory predictions using the current fields of IRENOM obtained with an initialization time at least of 5 days. However, the circulation pattern depicted in Fig. 8-a-b-c shows that a spin-up time longer than 3 days breaks the flow continuity that is observed along the channel, leading to worse trajectories predictions (presented later in this Sect.).

Fig. 8-d shows the sea surface current fields with a horizontal resolution of 2 km with a spin-up time of 3 days (5 days and 7 days spin-up time result are not shown) and forced by ECWMF 0.25° wind forcing. With this finer horizontal grid resolution different spatial scales develop in comparison to the coarser 3 km resolution. In particular, considering that at the time of drifters release a wind of about 5 m/s was blowing from north east, it is expected the development of weaker currents in the calm lee behind Elba island. This is actually the case for the finer grid resolution, in contrast to the current field observed in Fig. 8-a-b-c. The ratio between the Total Kinetic Energy (TKE), on the target day 14 February at 12:00 UTC, of the relocatable model with 2 km resolution and that of the father model MFS as a function of the spin-up time is shown in Fig. 9 (red line), with this resolution the slope of the curve is lower than with 3 km, suggesting that the plateau is almost reached after 3 days.

The sensitivity of the IRENOM configuration with 2 km resolution to the atmospheric model horizontal resolution has been also investigated and in Fig. 8-e the sea surface current fields, obtained with a spin-up time of 3 days, is shown (5 days and 7 days spin-up time result are not shown). With this finer wind forcing stronger westward currents develop south of the two islands and the current between the Giglio and Giannutri Island slightly changes its direction (eastward) compared to the currents presented in Fig. 8-d, leading to better trajectories predictions (presented later in this Sect.).

Furthermore, the model behavior related to initialization time, *IRENOM and atmospheric model horizontal resolution* is further investigated by comparing the model predicted Sea Surface Temperature (SST) to satellite radiometer

observations available from the MyOcean portal [64] as daily gap-free map at 1/16° resolution over the Mediterranean Sea. Fig. 10 shows the Root-Mean-Square-Error (RMSE) statistics as a function of spin-up time for 3 and 2 km grid resolution. *The HG2 configuration is in better agreement with observed SST, showing a lower RMSE than the HG1 configuration.* For both model configurations, there is a progressive increase of RMSE as a function of spin-up time, suggesting that shorter spin-up time should lead to lower error in SST estimates. We have to consider that the father model (MFS) current fields are analysis field, thus corrected using the assimilation of SST data. Thus, using a longer spin-up time we let the IRENOM model free to develop its own dynamics, but possibly introducing a greater uncertainty when the model moves away from the MFS initial conditions, as confirmed by the trajectories predictions (presented later in this Section) *As shown Fig. 10, the IRENOM configuration with 2 km resolution and forced by the 0.025°SKIRON wind is in better agreement with observed SST, showing a lower RMSE than the analogous configuration forced by the low resolution ECMWF wind..*

The IRENOM configurations has been then validated using the trajectories of the drifters released in the Costa Concordia accident area. Fig. 11-a shows the trajectory prediction for Buoy 1 using the IRENOM currents with resolution of 3 km and different spin-up times, forced by the ECMWF 0.25°wind. The best result is achieved with the IRENOM currents initialized 3 days before the drifter deployment, as shown in Tab. 5, lower separation distances and higher skill scores are obtained. While worst results are obtained increasing the spin-up time, although little difference in trajectory prediction are observed using a spin-up time of 5 or 7 days. As depicted in Fig. 8-a-b-c a spin-up time longer than 3 days breaks the flow continuity that is observed along the channel. This fact causes a worst trajectory prediction for Buoy 1, which follows a quite straight path across the channel. In summary, a greater spin-up time allows the generation of more spatial scales and stronger sea surface current, but introduces uncertainties in the current fields when the model moves away from the MFS initial conditions, that is corrected using data assimilation. Moreover, in this specific case longer spin-up time breaks the current which develops straight along the island's channel, leading to a worst trajectory prediction for Buoy 1.

Fig. 11-b shows the simulated trajectories using the IRENOM sea surface current with an horizontal resolution of 2 km and spin-up time of 7, 5 and 3 days, forced by the ECMWF 0.25°wind. The finer grid resolution allows the development of stronger current in the channel. As a consequence better trajectory prediction for Buoy 1 is achieved. The lowest separation distance after 24 hours, 2.88 km, and a skill score of 0.75, is achieved using 3 days of spin-up and 2 km of resolution. The spin-up time acts in the same way as for 3 km grid resolution. A 3 days spin-up time gives the best trajectory prediction, while longer spin-up times lead to a poorer trajectory prediction skill. In conclusion, it is suggested that the spin-up time for a relocatable model cannot be decided a priori and it should be a tuneable parameter.

Fig. 11-c shows the simulated trajectories using the IRENOM sea surface current with an horizontal resolution of 2 km and spin-up time of 7, 5 and 3 days, forced by the SKIRON 0.025° wind. To be consistent with the IRENOM current fields, the Stokes drift correction, $\mathbf{U}_S$ *of Eq. 7, and the wind drag correction,* $\mathbf{U}_D$ *of Eq. 5, are calculated by MEDSLIK-II using the SKIRON 0.025° wind field. The finer wind forcing produces the change in the direction of the current in the channel, that is now toward the east, as shown in Fig. 8-e. As a consequence better trajectory prediction for Buoy 1 is achieved. Although, the separation distance after 24 hours is 3.42 km, higher than in HG2-T11, it is qualitative evident that the modeled trajectory using the high resolution wind forcing is in better agreement with the observed trajectories. Indeed the highest skill score is obtained (0.79) and in this case, as suggested by Liu and Weisberg (2011), the separation distance might not be a good estimate of the trajectory accuracy. In conclusion, higher resolution wind forcing gives a better estimate of the simulated drifter path.*

Fig. 11-d shows the simulated trajectories using the MFS, TYRR and WMED currents in comparison with the trajectories obtained with IRENOM sea surface current forced by both the ECMWF 0.25°(HG2-T11) and SKIRON 0.025°(HG2-T11-SKI) with an horizontal resolution of 2 km, spin-up time of 3 days, which are the best ones among the IRENOM experiments. The IRENOM currents give the best results. We believe this is due to the correct topography (Giglio Island is correctly implemented in the model), to the initialization procedure with a spin-up time of 3 days. In the MFS model the Giglio Island is not reproduced and although in WMED and TYRR model the Giglio Island is correctly defined, problems can arise from the initizialization procedures: WMED has no spin-up time (cold start from MFS) and TYRR uses 7 days initialization period. *Furthermore, the higher resolution wind forcing further improves the modelled trajectories accuracy, while all the above operational models are forced by the ECMWF 0.25° forcing.*

In Tab. 5 the skills of the trajectory simulations obtained using the IRENOM model with the Shapiro filter applied on the bathymetry for the configuration with 2 km grid resolution (HG2-T11-YS) and using a lower shallowest topography vertical clipping of 5 m value (HG2-T11-C5) with respect to the 10 m used for all the other experiments are shown. There is a meaningless difference in drifter trajectory predictions with respect to the case where the bathymetry is not filtered (HG2-T11). As well as using a lower shallowest topography clipping of 5 m value does not provide meaningful differences in skill trajectory predictions.

Fig. 12 compares the trajectory predictions using the different IRENOM models configurations. It is evident that the trajectories of Buoys 2 and 3 are not correctly reproduced. This might be due to the incorrect positioning of vortex structures that affects the Buoy 2 and 3 movement. On the other hand, the presence of a baroclinic cyclonic vortex, that extends along the shelf, is shown in the IRENOM HG2-T11-SKI model configuration vorticity section (close to Buoy1 and 4 deploy position), see Fig. 13. This vortex might be cor-

rectly reproduced in the HG2-T11 configuration and influences the trajectory predictions of Buoy 1 and Buoy 4.

Besides the low performance of the IRENOM simulation in reproducing the Buoy 2 and 3, the overall skill scores, listed in Tab. 5, confirm that the best configuration is the experiment *HG2-T11-SKI with and overall skill score of 0.61. The mean separation distance appears to be lower in the HG2-T09-SKI*, but as suggested by Liu and Weisberg (2011), the separation distance might not be a good estimate of the trajectory accuracy, because looping trajectories may lead to an erroneous decrease of the separation distance, as it is the case of Buoy 4.

5 Summary and conclusions

In this paper, the scientific tools that can be used to aid during an environmental emergencies are utilized and studied, including an evaluation of their performances. The paper presented step by step the improvements that are taken to produce better ocean state prediction. The final outcome is that high resolution and accurate forecasts of the ocean currents that come from a relocatable ocean model (IRENOM) greatly improve the quality of the operational oceanography products*: our best results showed that the skill score in trajectory predictions (and the separation distance) is 0.79 (3.41 km) using the IRENOM model while using the coarser resolution model model is 0.28 (11.05 km)*. Such forecasts and estimates can be given to the competent authorities during environmental emergencies.

First, we introduced the results of the operational support given during the Costa Concordia emergency. We found that a multi-model approach can show some degree of confidence that any single model alone might not. When all the models are in agreement, we might be more confident in the accuracy of the forecasts. *Only a qualitative comparison of the model results has been performed and the different forecasts are not produced from true ensemble prediction systems based on dynamics. Despite this, a similar methodology was implemented during the Deepwater Horizon oil spill [52] [53] and it has demonstrated to provide some degree of confidence that any single model alone might not. One future solution would be to produce a unified daily product, that could be easily used by all responders. We might expect that somehow combining models might improve the trajectory estimates. Few examples on using ocean ensembles in Lagrangian trajectory models are available [104] [94] [109]. Those studies demonstrated that the ensemble can generate important uncertainty information in addition to predicting the drifter trajectory with higher probability, in contrast to a single ocean model forecast. More extensive new reasearch on using ocean ensmbles in Lagrangian trajectory predictions is expected in the near future.*

Second, the deployment of drifters showed to be a key instrument to evaluate the models performance, *as already demonstrated in other oil spill emergency cases [11] [50] [53] [57]*. The evaluation of the accuracy of the regional

MFS model and sub-regional WMED and TYRR models is perfomed by using the drifters trajectory predicted by the oil spill model, MEDSLIK-II. This experiments allowed to calibrate the MEDSLIK-II trajectory model configuration and we found that the best results are obtained using the Stokes drift and the wind drag correction. It has been found that the effect of wave and wind drag can be of the same order of magnitude of the currents velocity. We showed that using TYRR model with a resolution of 2 km, the lower separation distance between modelled and observed trajectories is 4.15 km and the higher skill score is 0.59.

Third, we presented how a relocatable modelling methodology can improve the ocean state prediction accuracy. The IRENOM relocatable model has been nested in the MFS operational products and its performances have been evaluated using drifters trajectories. It has been shown that thanks to the possibility to change easily and quickly its configuration, the IRENOM results were of greater accuracy than the results achieved using regional (MFS) or sub-regional products (WMED and TYRR). We found that the reproduction of the correct topography, taking into account the small islands, that in a low resolution model, such as MFS, are not correctly resolved, together with the initialization procedure are key configurations settings that should be correctly tuned. Regarding the initialization procedure, the general practice would suggest to choose the spin-up time which allows the ocean model to reach a state of physical equilibrium [95]. On the other hand, as we found in this work, using a longer spin-up time the IRENOM model is free to develop its own dynamics, but possibly introducing greater uncertainties when the model moves away form the MFS initial conditions (corrected using data assimilation). Thus, we can conclude that the spin-up time for a relocatable model cannot be decided a priori, but should be a tuneable parameter.

Furthermore, the IRENOM currents and the MEDSLIK-II simulated trajectories showed to be sensitive to the spatial resolution of the meteorological fields used, providing higher prediction skills with higher resolution wind forcing.. The best configurations of the IRENOM model are obtained using an initialization period of 3 days, a resolution of 2 km that allows the development of the stronger current in the channel between the two islands. *In addition, the SKIRON 0.025° wind allows to better reproduce the current direction inside the channel. With this configuration (2 km, 3 days spin-up, SKIRON 0.025°), the skill score [50] after 24 hours for the buoy located in between the two island (Buoy 1) is 0.79. On the other hand, with the same IRENOM configuration, two of the buoys were not correctly reproduced. This might be due to the incorrect positioning of vortex structures that affect the buoys movement. We believe that higher prediction skills might be achieved with increased resolution boundary conditions or two-way-nesting to resolve smaller spatial scales. Besides this, the results are still in agreement with the state-of-the-art literature, showing an average separation distance after 24 hours between 8.64 km, in agreement with the results found in the literature [16] [32] [50] [92], and the average skill score of 0.61.*

Finally, we should remark that few data were available for the models validation during the Costa Concordia emergency case. A specific protocol to acquire data necessary for the models validation in a short time framework should be developed and employed. Rapid environmental assessment methodology for rapid understanding of relevant environmental conditions at sea, in order to take tactical decisions, have been extensively developed in the past [27] and should be now adapted to the specific scopes of environmental emergencies. Thus, in the future, we should design and validate an innovative metholdogy for response to oil spill events, by using multi-platform observations (satellite, drifters, aerial surveys, CTD surveys) to improve the models forecast skill. The final aim should be the rapid analysis of environmental and oil pollution conditions in order to set up a specific protocol for response to oil spill pollution at sea.

References

1. Al-Rabeh, A. H., Lardner, R. W., and Gunay, N.: Gulfspill Version 2.0: a software package for oil spills in the Arabian Gulf, Environ. Modell. Softw., 15, 425–442, 2000.
2. Agarwal, A., Lermusiaux, P.F.J.: Statistical Field Estimation for Complex Coastal Regions and Archipelagos, Ocean Modeling, 40 (2), 164-189, 2011
3. Ambjörn, C.: Seatrack Web, Forecasts of Oil Spills, a New Version, Environ. Res. Eng. Manage., 3, 60–66, 2007.
4. ASA: OILMAP for Windows (technical manual), Narrangansett, Rhode Island: ASA Inc, 1997.
5. ASCE: State-of-the-Art Review of Modeling Transport and Fate of Oil Spills, J. Hydraulic Eng., 122, 594–609, 1996.
6. Auclair, F., Marsaleix, P., Estournel, C.:Sigma coordinate pressure gradient errors: Evaluation and reduction by an inverse method, Journal of Atmospheric and Oceanic Technology, 17(10), 13481367, 2000
7. Blain, C. A., Preller, R. H., Rivera, A. P.: Tidal prediction using the advanced circulation model (ADCIRC) and a relocatable PC-based system, Oceanography, 15(1), 77-87, 2002
8. Blumberg, A., Mellor, G.,: A description of a three-dimensional coastal ocean circulation model, Coastal Estuarine Science, N.S. Heaps Ed., Americ. Geophys. Union, Three-dimensional Coastal Ocean Models, 116, 1987.
9. Barron, C. N. and Smedstad, L. F. and Dastugue, J. M. and Smedstad, O. M.: Evaluation of ocean models using observed and simulated drifter trajectories: Impact of sea surface height on synthetic profiles for data assimilation, J. Geophys. Research, 112, C07019, 2007.
10. Berry, A., Dabrowski, T., and Lyons, K.: The oil spill model OILTRANS and its application to the Celtic Sea, Mar. Pollut. Bull., 2012.
11. Caballero, A., Espino, M., Sagarminaga, Y., Ferrer, L., Uriarte, A., González, M.: Simulating the migration of drifters deployed in the Bay of Biscay, during the Prestige crisis, Mar. Pollut. Bullet., 56, 475–482, 2008.
12. Carracedo, P., Torres-López, S., Barreiro, M., Montero, P., Balseiro, C. F., Penabad, E., Leitao, P.C., Pérez-Muñuzuri, V.: Improvement of pollutant drift forecast system applied to the *Prestige* oil spills in Galicia Coast (NW of Spain): Development of an operational system, Mar. Pollut. Bullet., 53(5), 350-360, 2006
13. Castanedo, S., Medina, R., Losada, I. J., Vidal, C., Mndez, F. J., Osorio, A., Juanes, J.A., Puente, A.: The Prestige oil spill in Cantabria (Bay of Biscay). Part I: operational forecasting system for quick response, risk assessment, and protection of natural resources, Journal of Coastal Research, 1474-1489, 2006
14. Castellari, S., Pinardi, N., Leaman, K.: A model study of air-sea interaction in the mediterranean sea. Journal of Marine System, 18, 89114, 1998

15. Coppini, G., M. De Dominicis, G. Zodiatis, R. Lardner, N. Pinardi, R. Santoleri, S. Colella, F. Bignami, D. R. Hayes, D. Soloviev, G. Georgiou, G. Kallos: Hindcast of oil-spill pollution during the Lebanon crisis in the Eastern Mediterranean, JulyAugust 2006. Mar. Pollut. Bullet., 62(1), 140-153, 2011
16. Cucco, A., Sinerchia, M., Ribotti, A., Olita, A., Fazioli, L., Perilli, A., Sorgente, B., Borghini, M., Schroeder, K., and Sorgente, R.: A high-resolution real-time forecasting system for predicting the fate of oil spills in the Strait of Bonifacio (western Mediterranean Sea), Mar. Pollut. Bullet., 64(6), 1186-1200, 2012.
17. Clementi, E., Oddo, P., Korres, G., Drudi, M., Pinardi, N., :Coupled wave-ocean modelling system in the Mediterranean Sea, 13th International Workshop on Wave Hindcasting and 4th Coastal Hazards Symposium, Alberta, Canada, 2013
18. Daniel, P., Josse, P., Dandin, P., Gouriou, V., Marchand, M., Tiercelin, C.: Forecasting the *Erika* oil spills, In International Oil Spill Conference, Vol. 2001, No. 1, pp. 649-655. American Petroleum Institute, 2001
19. Daniel, P., Marty, F., Josse, P., Skandrani, C., and Benshila, R.: Improvement of drift calculation in Mothy operational oil spill prediction system, in: International Oil Spill Conference (Vancouver, Canadian Coast Guard and Environment Canada), vol. 6, 2003.
20. De Dominicis, M., Leuzzi, G., Monti, P., Pinardi, N., and Poulain, P.: Eddy diffusivity derived from drifter data for dispersion model applications, Ocean Dynam., 1–18, 2012.
21. De Dominicis, M., Pinardi, N., and Zodiatis, G., Lardner, R.: MEDSLIK-II, a Lagrangian marine surface oil spill model for short-term forecasting – Part 1: Theory, Geosci. Model Dev., 6, 1851-1869, doi:10.5194/gmd-6-1851-2013, 2013.
22. De Dominicis, M., Pinardi, N., and Zodiatis, G., Archetti, R.: MEDSLIK-II, a Lagrangian marine surface oil spill model for short-term forecasting – Part 2: Numerical simulations and validations, Geosci. Model Dev., 6, 1871-1888, doi:10.5194/gmd-6-1871-2013, 2013.
23. Dietrich, D. E., Ko D. S., Yeske, L. A.: On the application and evaluation of the relocatable DieCAST ocean circulation model in coastal and semi-enclosed seas, Tech. Rep. 931, Center for Air Sea Technology, Mississippi State University, Stennis Space Center, MS, 1993.
24. Dietrich, J. C., Trahan, C. J., Howard, M. T., Fleming, J. G., Weaver, R. J., Tanaka, S., Yuf, L., Luettich Jr., R.A., Dawson, C.N., Westerink, J.J., Wells, G., Lu, A., Vega, K., Kubach, A., Dresback, K.M., Kolar, R.L., Kaiser, C., Twilley, R.R.: Surface trajectories of oil transport along the Northern Coastline of the Gulf of Mexico, Continental Shelf Research, 41, 17-47, 2012
25. Debreu, L., Blayo, E.: Two-way embedding algorithms: a review, Ocean Dynamics, 58(5-6), 415-428, 2008
26. Dobricic, S., Pinardi, N.: An oceanographic three-dimensional variational data assimilation scheme., Ocean Modelling, 22(3), 89-105, 2008.
27. Ferreira-Coelho, E., Rixen, M.: Maritime rapid environmental assessment new trends in operational oceanography, Journal of Marine Systems, 69 (12), 2008
28. Gaberšek, S. and Sorgente, R. and Natale, S. and Ribotti, A. and Olita, A. and Astraldi, M. and Borghini, M.:The Sicily Channel Regional Model forecasting system: initial boundary conditions sensitivity and case study evaluation. Ocean Science, 3, 3141, 2007.
29. Hackett, B., Breivik, Ø., and Wettre, C.: Forecasting the Drift of Objects and Substances in the Ocean, Ocean Weather Forecast., 507–523, 2006.
30. Haley Jr., P.J., Lermusiaux, P.F.J.: Multiscale two-way embedding schemes for free-surface primitive-equations in the Multidisciplinary Simulation, Estimation and Assimilation System, Ocean Dynamics, 60, 1497-1537, 2010
31. Haley Jr., P.J., Agarwal, A., Lermusiaux, P.F.J.: Optimizing Velocities and Transports for Complex Coastal Regions and Archipelagos, Ocean Modeling, 2013, submitted.
32. Huntley, H. S. and Lipphardt Jr, B. L. and Kirwan Jr, A. D.: Lagrangian predictability assessed in the East China Sea, Ocean Modelling, 36, 1, 163–178, 2011.
33. Isobe, A., Hinata, H., Shinichiro, K. A. K. O., Yoshioka, S.: Formulation of leeway-drift velocities for sea-surface drifting-objects based on a wind-wave flume experiment. Interdisciplinary Studies on Environmental Chemistry-Marine Environmental Modeling and Analysis, eds. K. Omori, X. Guo, N. Yoshie, N. Fujii, IC Handoh, A. Isobe and S. Tanabe, Terrapub., Tokyo, 239-249, 2011.

34. Jackson, J. B., Cubit, J. D., Keller, B. D., Batista, V., Burns, K., Caffey, H. M., Caldwell, R. L., Garrity, S. D., Getter, C. D., Gonzalez, C., Guzman, H. M., Kaufmann, K. W., Knap, A.H., Levings, S. C., Marshall, M. J., Steger, R., Thompson, R. C., Weil, E.: Ecological effects of a major oil spill on Panamanian coastal marine communities. Science, 243(4887), 37-44, 1989
35. Janjic, Z. I.: Nonlinear advection schemes and energy cascade on semi?staggered grids, Mon. Weather Rev., 112, 12341245, 1984
36. Kallos, G., Nickovic, S., Jovic, D., Kakaliagou, O., Papadopoulos, A., Misirlis, N., Boukas, L., Mimikou, N.: The ETA model operational forecasting system and its parallel implementation, 1st Workshop on Large?Scale Scientific Computations, Varna, Bulgaria, 711 June, 1997
37. Kallos, G., Papadopoulos, A., Katsafados, P., Nickovic, S.: Transatlantic Saharan dust transport: Model simulation and results, J. Geophys. Res., 111, D09204, 2006
38. Ko, D. S., Martin, P.J., Rowley, C.D., Preller, R.H.: A real-time coastal ocean prediction experiment for MREA04, Journal of Marine Systems, 69(1), 17-28, 2008
39. Krishnamurti, T. N., Kishtawal, C. M., Zhang, Z., LaRow, T., Bachiochi, D., Williford, E.: Multimodel ensemble forecasts for weather and seasonal climate, Journal of Climate, 13(23), 4196-4216, 2000.
40. Krishnamurti, T. N., Kishtawal, C. M., Shin, D. W., Williford, C. E.: Improving tropical precipitation forecasts from a multianalysis superensemble, Journal of climate, 13(23), 4217-4227, 2000.
41. Lardner, R., Zodiatis, G., Loizides, L., and Demetropoulos, A.: An operational oil spill model for the Levantine Basin(Eastern Mediterranean Sea), in: International Symposium on Marine Pollution, 1998.
42. Lardner, R., Zodiatis, G., Hayes, D., and Pinardi, N.: Application of the MEDSLIK Oil Spill Model to the Lebanese Spill of July 2006, European Group of Experts on Satellite Monitoring of Sea Based Oil Pollution, European Communities, 2006.
43. Lehr, W., Jones, R., Evans, M., Simecek-Beatty, D., and Overstreet, R.: Revisions of the ADIOS oil spill model, Environ. Modell. Softw., 17, 189–197, 2002.
44. Lermusiaux, P.F.J.: Estimation and study of mesoscale variability in the Strait of Sicily, Dynamics of Atmospheres and Oceans, 29, 255-303, 1999
45. Lermusiaux, P.F.J.: Uncertainty Estimation and Prediction for Interdisciplinary Ocean Dynamics. Special issue of on Uncertainty Quantification. J. Glimm and G. Karniadakis, Eds., Journal of Computational Physics, 217, 176-199, 2006
46. Lermusiaux, P. F., Haley Jr, P. J., Yilmaz, N. K.: Environmental prediction, path planning and adaptive sampling-Sensing and modeling for efficient ocean monitoring, management and pollution control, Sea Technology, 48(9), 35-38, 2007
47. Lermusiaux, P.F.J.: Adaptive Modeling, Adaptive Data Assimilation and Adaptive Sampling, Special issue on Mathematical Issues and Challenges in Data Assimilation for Geophysical Systems: Interdisciplinary Perspectives. C.K.R.T. Jones and K. Ide, Eds., Physica D, 230, 172196, 2007
48. Lermusiaux, P.F.J., Haley Jr., P.J., Leslie, W.G., Agarwal, A., Logutov, O., Burton, L.J.: Multiscale Physical and Biological Dynamics in the Philippines Archipelago: Predictions and Processes. Oceanography. PhilEx Issue, 24(1), 70-89, 2011
49. Leslie, W. G., Robinson, A. R., Haley Jr, P. J., Logutov, O., Moreno, P. A., Lermusiaux, P. F. J., Coelho, E.: Verification and training of real-time forecasting of multi-scale ocean dynamics for maritime rapid environmental assessment. Journal of Marine Systems, 69(1), 3-16, 2008.
50. Liu, Y., and Weisberg, R.H. 2011: Evaluation of trajectory modeling in different dynamic regions using normalized cumulative Lagrangian separation, J. Geophys. Res., 116, C09013, 2011b.
51. Liu, Y. and MacFadyen, A. and Ji, Z-G and Weisberg, R. H.: Introduction to Monitoring and Modeling the Deepwater Horizon Oil Spill, in Monitoring and Modeling the Deepwater Horizon Oil Spill: A Record-Breaking Enterprise, Geophys. Monogr. Ser., 195, 1–7, 2011a.
52. Liu, Y. and Weisberg, R. H. and Hu, C. and Zheng, L. : Tracking the Deepwater Horizon oil spill: A modeling perspective, Eos Trans. AGU, 92(6), 45-46, 2011c.
53. Liu, Y. and Weisberg, R. H. and Hu, C. and Zheng, L.: Trajectory forecast as a rapid response to the Deepwater Horizon oil spill, in Monitoring and Modeling the Deepwater

Horizon Oil Spill: A Record-Breaking Enterprise, Geophys. Monogr. Ser., 195, 153–165, 2011d.
54. Logutov, O.G. Lermusiaux, P.F.J.: Inverse Barotropic Tidal Estimation for Regional Ocean Applications, Ocean Modeling, 25, 17-34, 2008
55. Lozano, C.J., Robinson, A.R., Arango, H.G., Gangopadhyay, A., Sloan, Q., Haley, P.J., Anderson L., Leslie, W.: An interdisciplinary ocean prediction system: Assimilation strategies and structured data models, Elsevier Oceanography Series, 61, 413-452, 1996
56. Madec G.: NEMO ocean engine. Note du Pole de modélisation, Institut Pierre-Simon Laplace (IPSL), France, No 27, ISSN No 1288-1619, 2008
57. Mariano, A., Kourafalou, V., Srinivasan, A., Kang, H., Halliwell, G., Ryan, E., Roffer, M.: On the modeling of the 2010 Gulf of Mexico Oil Spil, Dynam. Atmos. Oceans, 2011.
58. Mason, E., Molemaker, J., Shchepetkin, A. F., Colas, F., McWilliams, J. C., Sangrá, P.: Procedures for offline grid nesting in regional ocean models, Ocean Modelling, 35(1), 1-15, 2010
59. MEDSLIK-II website: http://gnoo.bo.ingv.it/MEDSLIKII
60. Mellor, G. L., Yamada, T.:Development of a turbulence closure sub- model for geophysical fluid problems. Rev. Geophys. Space Phys. 20, 851 875, 1982.
61. Mellor, G. L.: User's Guide for a Three-Dimensional, Primitive Equation Numerical Ocean Model, Int. Rep., Program in Atmos. Ocean Sci., pp. 1135, Princeton Univ., Princeton, N. J., 2004
62. Mesinger, F.: A blocking technique for representation of mountains in atmospheric models, Riv. Meteorol. Aeronaut., 44, 195202, 1984
63. Mediterranen Forecasting System website: http://gnoo.bo.ingv.it/mfs/myocean/
64. MyOcean website: http://www.myocean.eu/
65. Nittis, K., Perivoliotis, L., Korres, G., Tziavos, C., and Thanos, I.: Operational monitoring and forecasting for marine environmental applications in the Aegean Sea, Environ. Modell. Softw., 21, 243–257, 2006.
66. Oddo, P., Adani, M., Pinardi, N., Fratianni, C., Tonani, M., Pettenuzzo, D.: A nested Atlantic-Mediterranean Sea general circulation model for operational forecasting., Ocean Science, 5(4), 461, 2009.
67. Olita A., Ribotti, A., Fazioli, L., Perilli, A., R. Sorgente: Surface circulation and upwelling in the western Sardinia sea: a numerical study, Continental Shelf Research, 71, 95-108, 2013
68. Onken R., Robinson, A.R., Lermusiaux, P.F.J., Haley Jr., P.J., Anderson, L.A.: Data-driven simulations of synoptic circulation and transports in the Tunisia-Sardinia-Sicily region, J. of Geophysical Research, 108, (C9), 8123-8136, 2002
69. Onken, R., Robinson, A. R., Kantha, L., Lozano, C. J., Haley, P. J., Carniel, S.: A rapid response nowcast/forecast system using multiply nested ocean models and distributed data systems. Journal of Marine Systems, 56(1), 45-66, 2005
70. Orlanski, I.: A simple boundary condition for unbounded hyperbolic flows., Journal of computational physics, 21(3), 251-269, 1976
71. Posey, P. G., Allard, R. A., Preller, R. H., Dawson, G. M.: Validation of the Global Relocatable Tide/Surge Model PCTides, Journal of Atmospheric and Oceanic Technology, 25:5, 755-775, 2008
72. Peterson, C. H., Rice, S. D., Short, J. W., Esler, D., Bodkin, J. L., Ballachey, B. E., Irons, D. B.: Long-term ecosystem response to the Exxon Valdez oil spill, Science, 302(5653), 2082-2086, 2003
73. Piatt, J. F., Anderson, P.: Response of common murres to the Exxon Valdez oil spill and long-term changes in the Gulf of Alaska marine ecosystem. In: American Fisheries Society Symposium, Vol. 18, pp. 720-737, 1996
74. Pollani, A., Triantafyllou, G., Petihakis, G., Nittis, K., Dounas, C., and Christoforos, K.: The Poseidon operational tool for the prediction of floating pollutant transport, Mar. Pollut. Bull., 43, 270–278, 2001.
75. Pinardi, N. and Coppini, G.: Preface "Operational oceanography in the Mediterranean Sea: the second stage of development", Ocean Sci., 6, 263–267,http://dx.doi.org/10.5194/os-6-263-2010, 2010.
76. Price, J. M., Reed, M., Howard, M. K., Johnson, W. R., Ji, Z. G., Marshall, C. F., Guinasso, N. L., and Rainey, G. B.: Preliminary assessment of an oil-spill trajectory model

using satellite-tracked, oil-spill-simulating drifters, Environ. Model. Softw., 21, 258–270, 2006.
77. Proctor, R., Elliot, A. J., Flather, R. A.:Forecast and hindcast simulations of the¡ i¿ Braer¡/i¿ oil spill, Mar. Pollut. Bullet., 28(4), 219-229, 1994
78. Ramp, S.R., Lermusiaux, P.F.J., Shulman, I., Chao, Y., Wolf, R.E., Bahr, F.L.: Oceanographic and Atmospheric Conditions on the Continental Shelf North of the Monterey Bay during August 2006, Dynamics of Atmospheres and Oceans, 52, 192-223, 2011
79. Reed, M., Gundlach, E., and Kana, T.: A coastal zone oil spill model: development and sensitivity studies, Oil Chem. Pollut., 5, 411–449, 1989.
80. Reed, M., Johansen, Ø., Brandvik, P. J., Daling, P., Lewis, A., Fiocco, R., Mackay, D., and Prentki, R.: Oil Spill Modeling towards the Close of the 20th Century: Overview of the State of the Art, Spill Sci. Technol. Bull., 5, 3–16, 1999.
81. Reed, M., Turner, C., and Odulo, A.: The role of wind and emulsification in modelling oil spill and surface drifter trajectories, Spill. Sci. Technol. B., 1, 143–157, 1994.
82. Reed, M., Aamo, O. M., and Daling, P. S.: Quantitative analysis of alternate oil spill response strategies using OSCAR, Spill Sci. Technol. Bull., 2, 67–74, 1995.
83. Rixen, M., Ferreira-Coelho, E.: Operational surface drift prediction using linear and non-linear hyper-ensemble statistics on atmospheric and ocean models, Journal of Marine Systems, 65(1), 105-121, 2007
84. Rixen, M., Ferreira-Coelho, E., Signell, R.: Surface drift prediction in the Adriatic Sea using hyper-ensemble statistics on atmospheric, ocean and wave models: uncertainties and probability distribution areas, Journal of Marine Systems, 69(1), 86-98, 2008
85. Rixen M., Book J., Carta A., Grandi V., Gualdesi L., Stoner R., Ranelli P., Cavanna A., Zanasca P., Baldasserini G., Trangeled A., Lewis C., Trees C., Grasso R., Giannechini S., Fabiani A., Merani D., Berni A., Leonard M., Martin P., Rowley C., Hulbert M., Quaid A., Goode W., Preller R., Pinardi N., Oddo P., Guarnieri A., Chiggiato J., Carniel S., Russo A., Tudor M., Lenartz F., Vandenbulcke L.: Improved ocean prediction skill and reduced uncertainty in the coastal region from multi-model super-ensembles, Journal of Marine Systems, 78, S282-S289, 2009
86. Robinson, A.R., Arango, H.G., Miller, A.J., Warn-Varnas, A., Poulain, P.M., Leslie, W.G.: Real-Time Operational Forecasting on Shipboard of the Iceland-Faeroe Frontal Variability, Bulletin of the American Meteorological Society, 72 (2), 243-259, 1996
87. Robinson, A.R., Sellschopp, J., Warn-Varnas, A., Leslie, W.G., Lozano, C.J., Haley Jr., P.J., Anderson, L.A., Lermusiaux, P.F.J.: The Atlantic Ionian Stream, Journal of Marine Systems, 20, 129-156, 1999
88. Robinson, A.: Forecasting and simulating coastal ocean processes and variabilities with the Harvard Ocean Prediction System, Coastal Ocean Prediction, AGU Coastal and Estuarine Studies Series, Am. Geophys. Union, 77–100, 1999.
89. Robinson, A.R, Sellschopp, J.: Rapid Assessment of the Coastal Ocean Environment. Ocean Forecasting: Conceptual Basis and Applications. N. Pinardi & J.D.Woods (editors), Springer, 203-232, 2002
90. Robinson, A.R., Haley, P.J., Lermusiaux, P.F.J., Leslie, W.G.: Predictive skill, predictive capability and predictability in ocean forecasting, Proceedings of the "The OCEANS 2002 MTS/IEEE" conference, Holland Publications, 787-794, 2002
91. Robinson, A.R., Sellschopp, J., Leslie, W.G., Alvarez, A., Baldasserini, G., Haley, P.J., Lermusiaux, P.F.J., Lozano, C.J., Nacini, E., Onken, R., Stoner, R., Zanasca, P.: Forecasting synoptic transients in the Eastern Ligurian Sea, In "Rapid Environmental Assessment", Bovio, E., R. Tyce and H. Schmidt (Editors), SACLANTCEN Conference Proceedings Series CP-46, Saclantcen, La Spezia, Italy, 2003
92. Röhrs, J. and Christensen, K. H. and Hole, L. R. and Broström, G. and Drivdal, M. and Sundby, S.: Observation-based evaluation of surface wave effects on currents and trajectory forecasts, Ocean Dynamics, 62, 10-12, 1519–1533, 2012.
93. Russo A., Coluccelli, A.: Integration of a relocatable ocean model in the Mediterranean Forecasting System, Ocean Sci. Discuss., 3, 16091621, 2006.
94. Scott, R. B., Ferry, N., Drévillon, M., Barron, C. N., Jourdain, N. C., Lellouche, J. M., Metzger, E.J., Rio, M., Smedstad, O. M.: Estimates of surface drifter trajectories in the equatorial Atlantic: a multi-model ensemble approach, Ocean Dynamics, 62(7), 1091-1109, 2012

95. Simoncelli, S., Pinardi, N., Oddo, P., Mariano, A. J., Montanari, G., Rinaldi, A., and Deserti, M.: Coastal Rapid Environmental Assessment in the Northern Adriatic Sea. Dynamics of atmospheres and oceans, 52(1), 250-283, 2011
96. Smagorinsky, J.:Some historical remarks on the use of nonlinear viscosities, in Large eddy simulations of complex engineering and geophysical flows, Galperin, B. and Orszag., S. Eds., 1, 69-106, 1993.
97. Sorgente, R., Drago, A. F., Ribotti, A.: Seasonal variability in the central mediterranean sea circulation. Annales Geophysicae, 21, 299322, 2003.
98. Sotillo, M., Alvarez Fanjul, E., Castanedo, S., Abascal, A., Menendez, J., Emelianov, M., Olivella, R., García-Ladona, E., Ruiz-Villarreal, M., Conde, J., Gǿomez, M., Conde, P., Gutierrez, A., and Medina, R.: Towards an operational system for oil-spill forecast over Spanish waters: Initial developments and implementation test, Mar. Pollut. Bull., 56, 686–703, 2008.
99. Spaulding, M., Kolluru, V., Anderson, E., and Howlett, E.: Application of three-dimensional oil spill model (WOSM/OILMAP) to hindcast the Braer spill, Spill Sci. Technol. Bull., 1, 23–35, 1994.
100. Spyrou, C., Mitsakou, C. ,Kallos, G. , Louka, P., Vlastou, G.: An improved limited area model for describing the dust cycle in the atmosphere, J. Geophys. Res., 115, D17211, 2010.
101. Thyrrenian Forecasting system website: http://utmea.enea.it/research/MEDMOD/
102. Tolman, H.L. :User manual and system documentation of WAVEWATCH III version 3.14., NOAA/NWS/NCEP/MMAB Tech. Note 276, 194 pp, 2009
103. Tonani, M., Pinardi, N., Dobricic, S., Pujol, I., and Fratianni, C.: A high-resolution free-surface model of the Mediterranean Sea, Ocean Sci., 4, 1–14, http://dx.doi.org/10.5194/os-4-1-2008, 2008.
104. Vandenbulcke, L., Beckers, J. M., Lenartz, F., Barth, A., Poulain, P. M., Aidonidis, M., Meyrat, J. , Ardhuin, F. , Tonani, M., Fratianni, C., Torrisi, L., Pallela, D., Chiggiato, J., Tudor, M. , Book, J.W., Martin, P., Peggion, G., Rixen, M.: Super-ensemble techniques: Application to surface drift prediction, Progress in Oceanography, 82(3), 149-167, 2009
105. Vetrano, A., Napolitano, E., Iacono, R., Schroeder, K., Gasparini, G. P.: Tyrrhenian Sea circulation and water mass fluxes in spring 2004: Observations and model results., Journal of Geophysical Research: Oceans (19782012), 115(C6), 2010.
106. Wang, J. and Shen, Y.: Development of an integrated model system to simulate transport and fate of oil spills in seas, Sci. China Technol. Sci., 53, 2423–2434, 2010.
107. Wang, S., Shen, Y., Guo, Y., and Tang, J.: Three-dimensional numerical simulation for transport of oil spills in seas, Ocean Eng., 35, 503–510, 2008.
108. Wei, M., Jacobs, G., Rowley, C., Barron, C. N., Hogan, P., Spence, P., Smedstad, O.M., Martin, P., Muscarella, P., Coelho, E.: The impact of initial spread calibration on the RELO ensemble and its application to Lagrangian dynamics, Nonlinear Processes in Geophysics, 20, 621-641, 2013
109. Wei, M., Jacobs, G., Rowley, C., Barron, C. N., Hogan, P., Spence, P., Smedstad, O.M., Martin, P., Muscarella, P. Coelho, E.: The performance of the US Navy's RELO ensemble, NCOM, HYCOM during the period of GLAD at-sea experiment in the Gulf of Mexico. Deep Sea Research Part II: Topical Studies in Oceanography, 2013
110. Western Mediterranean Forecasting system website: http://www.seaforecast.cnr.it/en/fl/wmed.php
111. Xie, P., Arkin, P. A.:Global Precipitation: A 17-Year Monthly Analysis Based on Gauge Observations, Satellite Estimates, and Numerical Model Outputs,Bulletin of the American Meteorological Society, 11, 2539–2558, 1997
112. Zelenke, B., C. O'Connor, C. Barker, C.J. Beegle-Krause, and L. Eclipse (Eds.): General NOAA Operational Modeling Environment (GNOME) Technical Documentation. U.S. Dept. of Commerce, NOAA Technical Memorandum NOS OR&R 40. Seattle, WA: Emergency Response Division, NOAA. 105 pp, http://response.restoration.noaa.gov/gnome_manual, 2012.

Table 1 OGCMs characteristics and domains.

Model Name	Domain	Resolution	Numerical Code	Father model
MFS	-6.0°E - 36.25°E; 30.25°N - 46.0°N	1/16°	NEMO	-
TYRR	8.81°E - 16.29°E; 36.68°N - 44.5°N	1/48°	POM	MFS
WMED	3.0°E - 16.47°E; 36.7°N - 44.48°N	1/32°	POM	MFS
IRENOM-HG1	9.11°E - 12.73°E; 41.26°N - 43.93°N	1/27°(Lon) - 1/37°(Lat)	HOPS	MFS
IRENOM-HG2	9.39°E - 12.29°E; 41.70°N - 43.12°N	1/41°(Lon) - 1/56°(Lat)	HOPS	MFS

Table 2 Sensitivity experiments of modeled trajectories to different OGCMs currents fields and to the particle trajectory equation terms.

Exp. Name	Current field	$\mathbf{U}_C$	$\mathbf{U}_S$	$\mathbf{U}_W$	$\mathbf{U}_D$
MFS-C	Hourly Surface Currents MFS	YES	NO	NO	NO
WMED-C	Hourly Surface Currents WMED	YES	NO	NO	NO
TYRR-C	Hourly Surface Currents TYRR	YES	NO	NO	NO
MFS-CS	Hourly Surface Currents MFS	YES	YES	NO	NO
WMED-CS	Hourly Surface Currents WMED	YES	YES	NO	NO
TYRR-CS	Hourly Surface Currents TYRR	YES	YES	NO	NO
MFS-CSD	Hourly Surface Currents MFS	YES	YES	NO	YES
WMED-CSD	Hourly Surface Currents WMED	YES	YES	NO	YES
TYRR-CSD	Hourly Surface Currents TYRR	YES	YES	NO	YES

Table 3 Results in terms of separation distances and skill scores.

Exp. Name	Buoy1 d_{24h}	Buoy1 ss_{24h}	Mean d_{24h}	Mean ss_{24h}
MFS-C	16.73 km	0	14.93 km	0.09
WMED-C	23.06 km	0	20.56 km	0
TYRR-C	9.34 km	0.35	13.16 km	0.33
MFS-CS	13.68 km	0.15	11.78 km	0.30
WMED-CS	20.15 km	0	15.93 km	0.13
TYRR-CS	6.10 km	0.50	11.51 km	0.48
MFS-CSD	11.05 km	0.28	9.55 km	0.46
WMED-CSD	17.63 km	0.06	13.01 km	0.35
TYRR-CSD	**4.15 km**	**0.59**	10.34 km	**0.54**

Table 4 Sensitivity experiments with IRENOM to different model settings.

Exp. Name	Horiz. Resol.	Spin-up	Vertic. Clipp.	Shapiro	Wind Forcing
HG1-T11	3 km	3 days	10 m	NO	ECMWF 0.25°
HG1-T09	3 km	5 days	10 m	NO	ECMWF 0.25°
HG1-T07	3 km	7 days	10 m	NO	ECMWF 0.25°
HG2-T11	2 km	3 days	10 m	NO	ECMWF 0.25°
HG2-T09	2 km	5 days	10 m	NO	ECMWF 0.25°
HG2-T07	2 km	7 days	10 m	NO	ECMWF 0.25°
HG2-T11-YS	2 km	3 days	10 m	YES	SKIRON 0.025°
HG2-T11-C5	2 km	3 days	5 m	NO	SKIRON 0.025°
HG2-T11-SKI	2 km	3 days	10 m	NO	SKIRON 0.025°
HG2-T09-SKI	2 km	5 days	10 m	NO	SKIRON 0.025°
HG2-T07-SKI	2 km	7 days	10 m	NO	SKIRON 0.025°

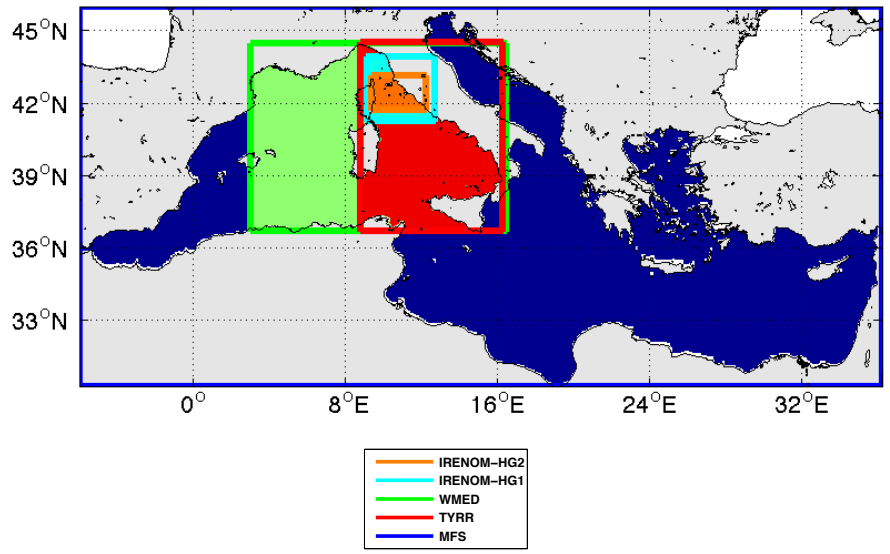

Fig. 1 OGCMs domains: the blue box is the MFS domain with 6.5 km resolution, the green box is the WMED domain with 3.5 km resolution, the red box is the TYRR domain with 2 km resolution, the light blue box is the IRENOM-HG1 domain with 3 km resolution and the orange box is the IRENOM-HG2 domain with 2 km resolution (the zoom of the IRENOM domains is in Fig. 2). *Coastline data from GSHHG (Global Self-consistent, Hierarchical, High-resolution Geography Database).*

Table 5 Relocatable model perfomances in terms of trajectories separation distances and skill scores.

Exp. Name	Buoy1 d_{24h}	Buoy1 ss_{24h}	Mean d_{24h}	Mean ss_{24h}
HG1-T11	3.60 km	0.66	10.47 km	0.53
HG1-T09	6.39 km	0.57	11.56 km	0.48
HG1-T07	7.75 km	0.51	11.24 km	0.49
HG2-T11	**2.88 km**	0.75	10.06 km	0.59
HG2-T09	3.78 km	0.67	9.02 km	0.59
HG2-T07	4.78 km	0.62	8.87 km	0.58
HG2-T11-YS	2.87 km	0.74	10.15 km	0.58
HG2-T11-C5	3.16 km	0.75	10.21 km	0.57
HG2-T11-SKI	3.41 km	**0.79**	8.64 km	**0.61**
HG2-T09-SKI	5.96 km	0.59	7.82 km	0.56
HG2-T07-SKI	7.39 km	0.55	9.80 km	0.44

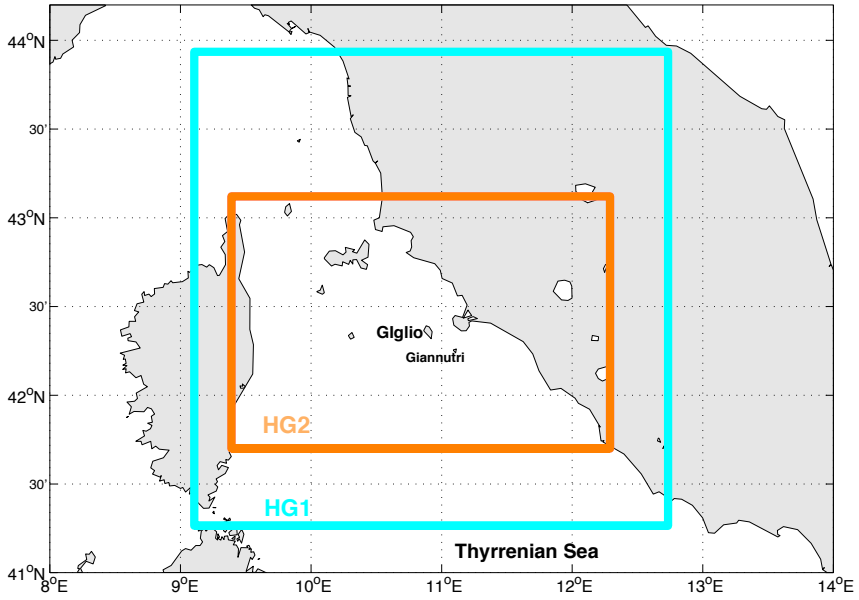

Fig. 2 IRENOM domains: the light blue box is the IRENOM domain with 3 km resolution identified by the label HG1 and the orange box is the IRENOM domain with 2 km resolution identified by the label HG2. *Coastline data from GSHHG (Global Self-consistent, Hierarchical, High-resolution Geography Database).*

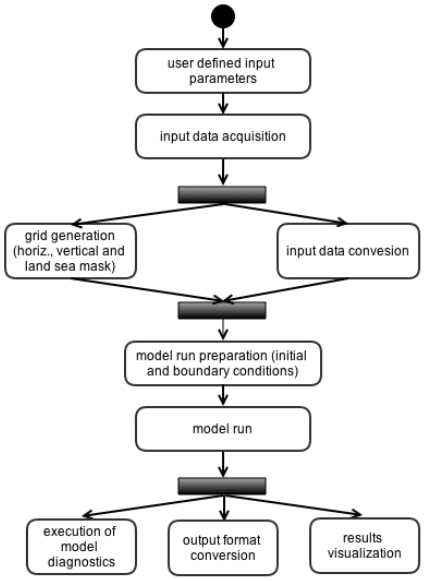

Fig. 3 Flowchart of the IRENOM implementation trough the GUI.

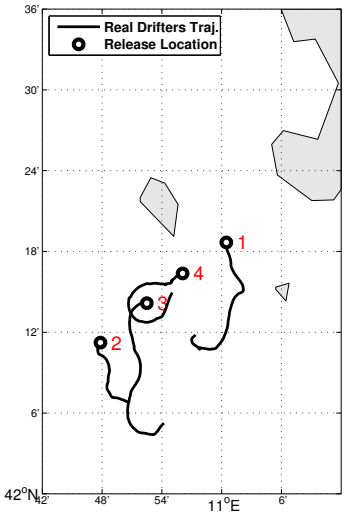

Fig. 4 Real drifters trajectories (black lines) from 14th February at 9:00 UTC to 15th February at 9:00 UTC.

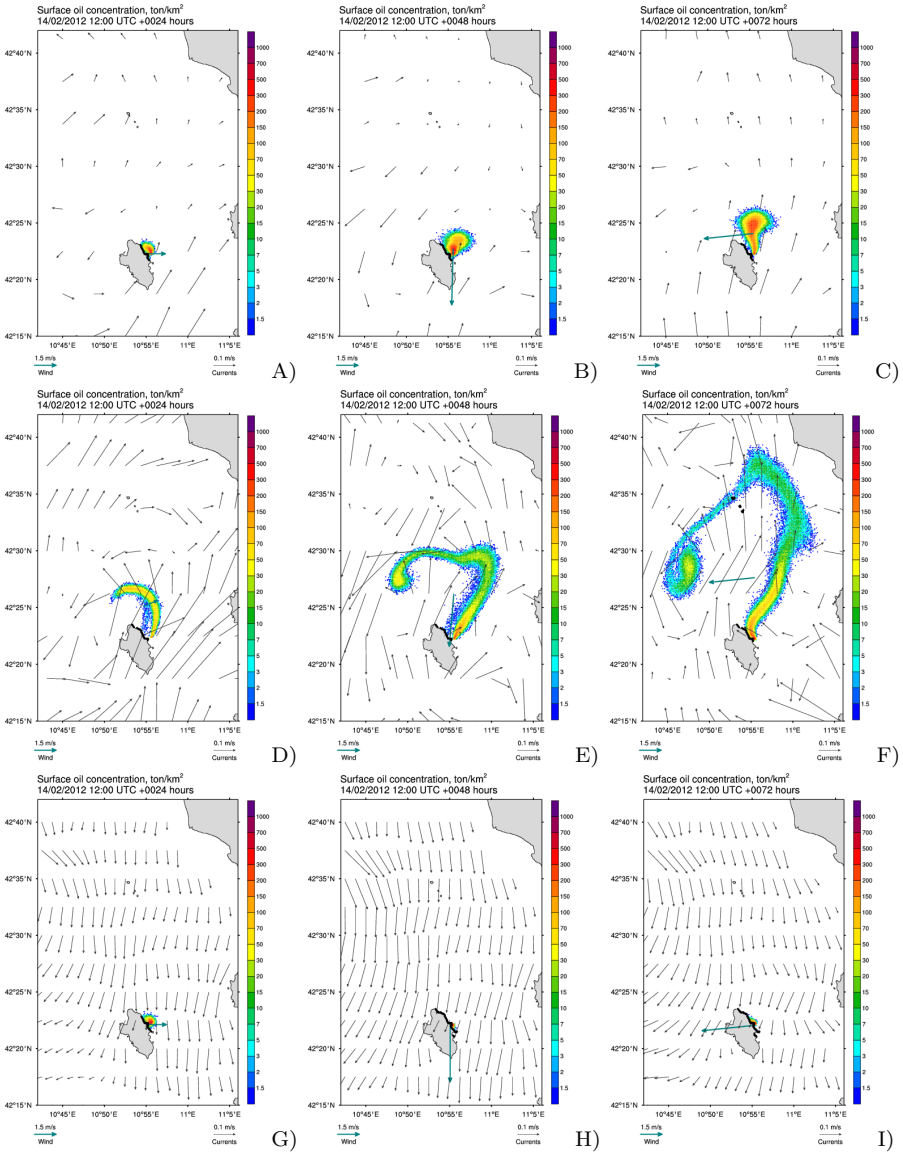

Fig. 5 The 14th of February 2012 bulletin example: the surface oil concentration 24 hours, 48 hours and 72 hours after the possible spill using MFS (A-B-C), WME (C-D-E) and TYRR (G-H-I). Oil concentration is visualized with colors from blue to purple in ton/km^2. Oil on the coast is highlighted in black. Currents (black arrows) and wind (green arrow) forecasts are shown in the background.

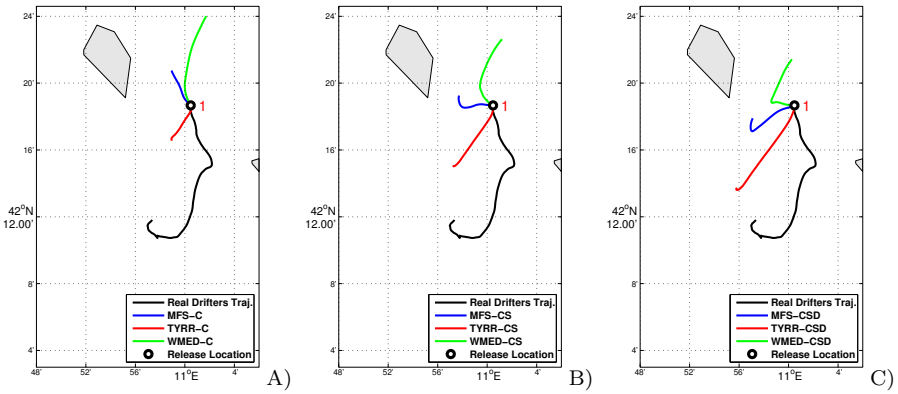

Fig. 6 Drifter 1 observed trajectory (black line) and the MEDSLIK-II trajectories using MFS (blues lines), WMED (green lines) and TYRR (red lines). Panel (A): using only the surface current term; Panel (B): using the surface current term and the Stokes drift correction; Panel (C): using the surface current term, the Stokes drift and the wind drag.

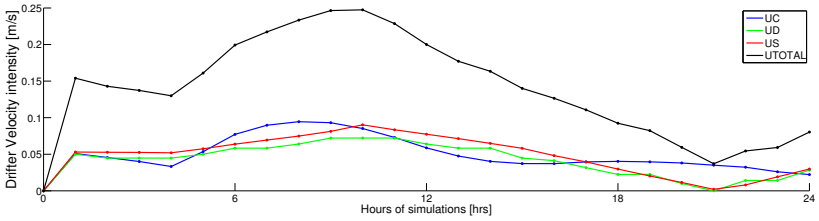

Fig. 7 Decomposition in its three components (currents, Stokes drift and wind drag) of the total velocity intensity used in Exp. TYRR-CSD.

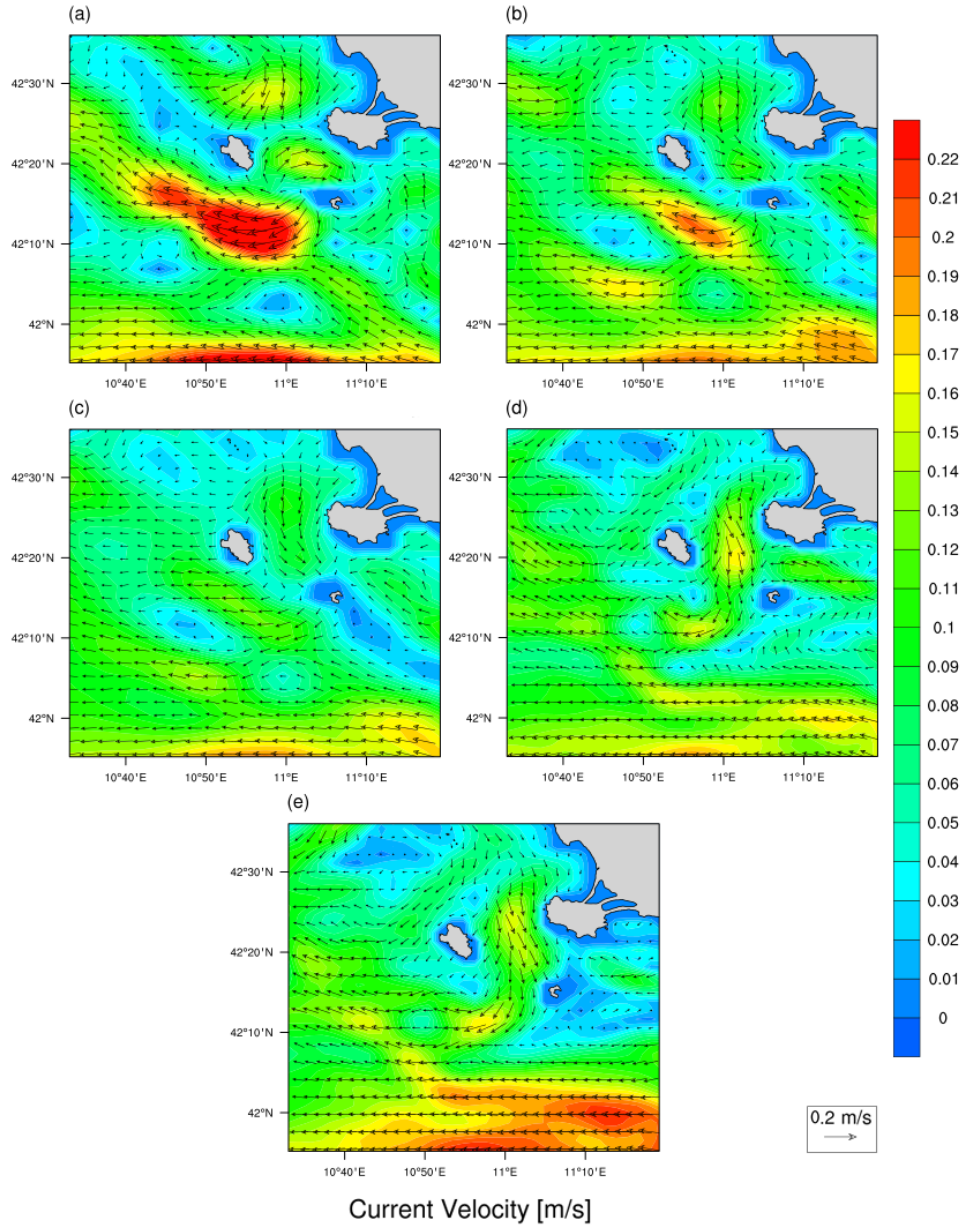

Fig. 8 Sensitivity of the IRENOM current fields to the spin-up time, model numerical horizontal grid resolution and wind forcing horizontal resolution. Currents field at the 14 February 2012 12:00 UTC: 7 days spin-up - 3 km - ECMWF 0.25°(panel a), 5 days spin-up - 3 km - ECMWF 0.25°(panel b), 3 days spin-up - 3 km - ECMWF 0.25°(panel c), 3 days spin-up - 2 km - ECMWF 0.25°(panel d) and 3 days spin-up - 2 km - SKIRON 0.025°.

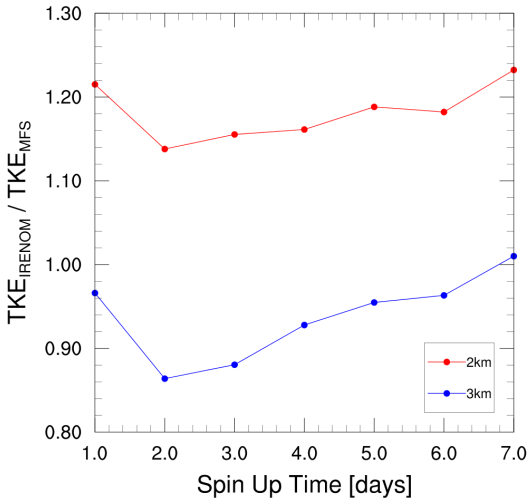

Fig. 9 Mean kinetic energy ratio between IRENOM relocatable model and MFS father model calculated on target day 14 February 12:00 UTC as function of spin-up time.

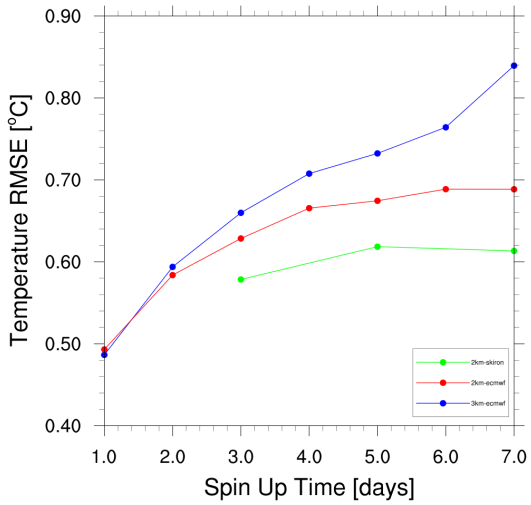

Fig. 10 Temperature RMSE calculated on day 14 February 12:00 UTC as function of spin-up time.

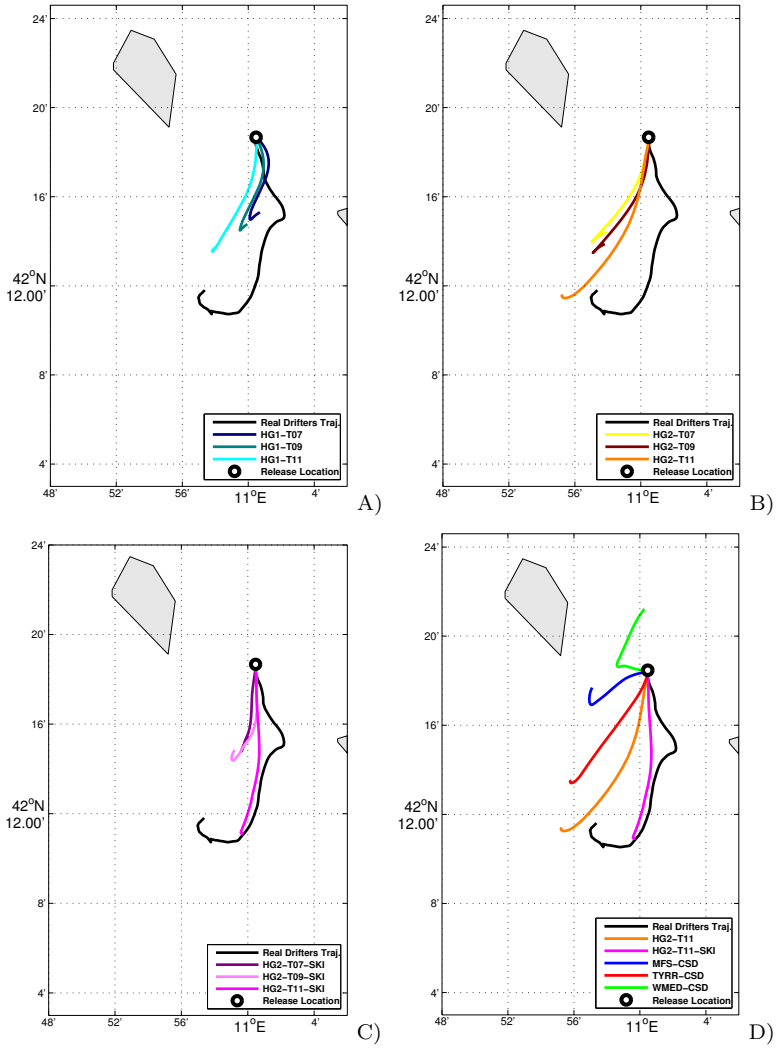

Fig. 11 Simulated drifter trajectories using the IRENOM currents. Panel a): Horizontal resolution 3 km, with a spin-up time of 7 days (HG1-T07), 5 days (HG1-T09) and 3 days (HG1-T11). Panel b) Horizontal resolution of 2 km, with a spin-up time of 7 days (HG2-T07), 5 days (HG2-T09) and 3 days (HG2-T11). Panel c) Horizontal resolution of 2 km and SKIRON wind forcing (0.025°) with a spin-up time of 7 days (HG2-T07-SKI), 5 days (HG2-T09-SKI) and 3 days (HG2-T11-SKI). Panel d) Comparison between the simulated drifters obtained with the MFS, WMED, TYRR and IRENOM currents with spin-up time (3 days), resolution 2 km and SKIRON wind forcing (HG2-T11-SKI)

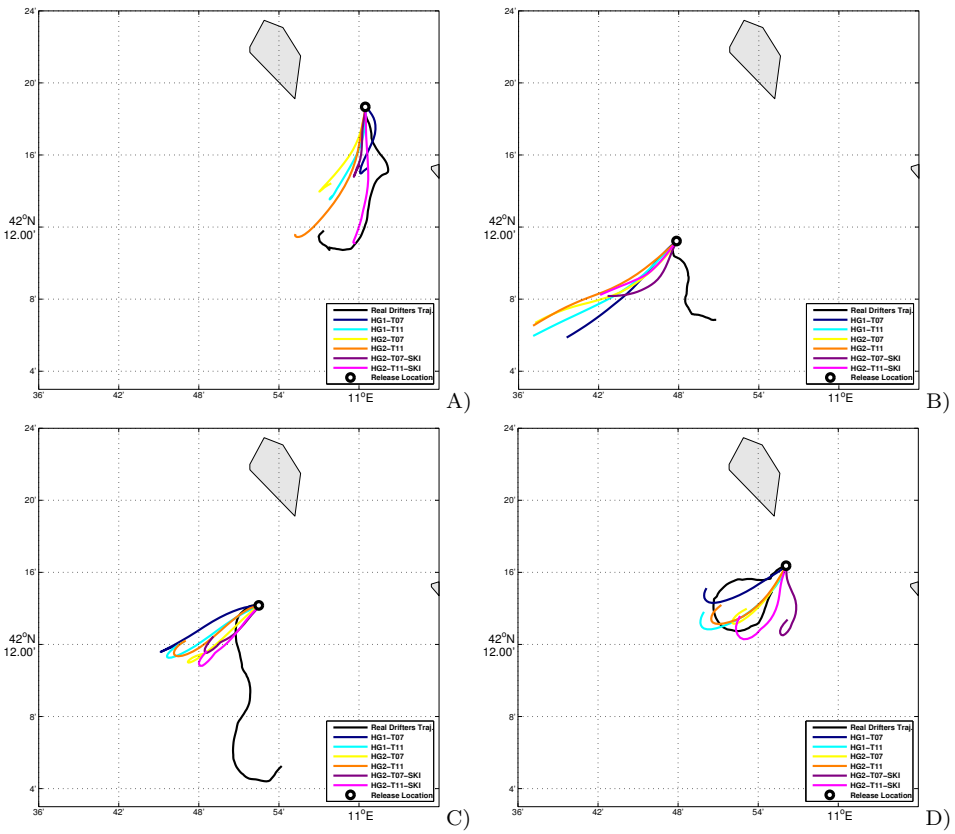

Fig. 12 Trajectory predictions using the different IRENOM models configurations: A) Buoy 1; B) Buoy 2; C) Buoy 3 and D) Buoy 4.

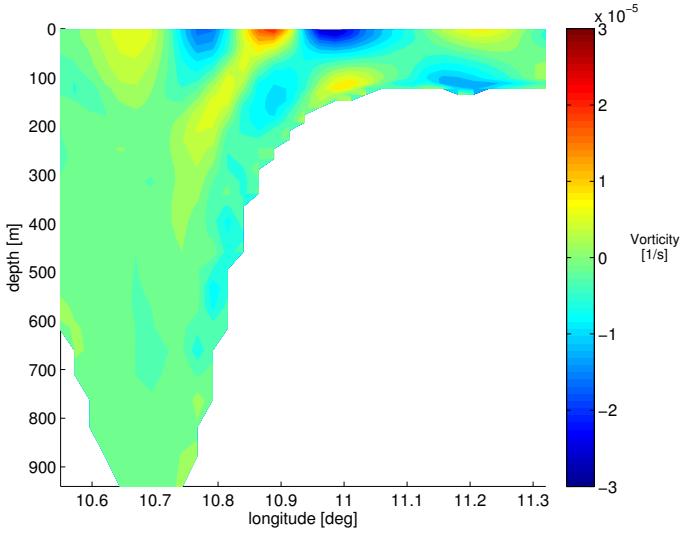

Fig. 13 Zonal vorticity section at 42.16°N of the IRENOM model with 2 km of resolution, 3 days of spin-up time and forced by SKIRON 0.025°(HG2-T11-SKI). A baroclinic cyclonic vortex extends along the shelf.